

# Selective Catalytic Deuterium Labeling of Alcohols during a Transfer Hydrogenation Process of Ketones Using D<sub>2</sub>O as the Only Deuterium Source. Theoretical and Experimental Demonstration of a Ru–H/D<sup>+</sup> Exchange as the Key Step

M. Carmen Carrión,<sup>†,‡</sup> Margarita Ruiz-Castañeda,<sup>†</sup> Gustavo Espino,<sup>§</sup> Cristina Aliende,<sup>§</sup> Lucía Santos,<sup>⊥</sup> Ana M. Rodríguez,<sup>¶</sup> Blanca R. Manzano,<sup>†</sup> Félix A. Jalón,<sup>\*,†</sup> and Agustí Lledós<sup>\*,||</sup>

<sup>†</sup>Departamento de Química Inorgánica, Orgánica y Bioquímica, UCLM. Facultad de Ciencias y Tecnologías Químicas-IRICA, Avda. C. J. Cela, 10, 13071 Ciudad Real, Spain

<sup>‡</sup>Fundación PCYTA, Paseo de la innovación, 1, 02006 Albacete, Spain

<sup>§</sup>Departamento de Química, Facultad de Ciencias, Univ. de Burgos. Plaza Misael Bañuelos s/n, 09001 Burgos, Spain

<sup>⊥</sup>Departamento de Química Física, UCLM. Facultad de Ciencias y Tecnologías Químicas, Avda. C. J. Cela, s/n, 13071 Ciudad Real, Spain

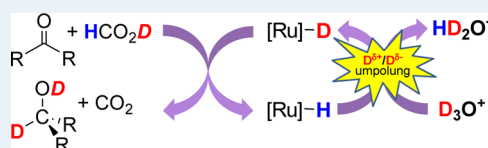
<sup>¶</sup>Departamento de Química Inorgánica, Orgánica y Bioquímica, UCLM, Escuela Técnica Superior de Ingenieros Industriales, Avda. C. J. Cela, 3, 13071 Ciudad Real, Spain

<sup>||</sup>Departament de Química, Universitat Autònoma de Barcelona, Edifici Cn, 08193 Cerdanyola del Vallés, Spain

## Supporting Information

**ABSTRACT:** The new complex  $[(\eta^6\text{-}p\text{-cym})\text{RuCl}(\kappa^2\text{-}N,N\text{-dmbpy})](\text{BF}_4)$  ( $p\text{-cym}$  =  $p$ -cymene;  $\text{dmbpy}$  = 4,4'-dimethyl-2,2'-bipyridine) is water-soluble and active in the catalytic transfer hydrogenation (TH) of different ketones (cyclohexanone, 2-cyclohexenone, and 3-pentanone) to the corresponding alcohols using aqueous  $\text{HCOONa}/\text{HCOOH}$  as the hydrogen source at pH 4.4. A higher activity was found for the TH of the imine  $N$ -benzylideneaniline under the same conditions. Excellent results have been obtained for catalyst recycling. Aqua, formato, and hydrido species were detected by  $^1\text{H}$  NMR experiments in  $\text{D}_2\text{O}$ . Importantly, when the catalytic reaction was carried out in  $\text{D}_2\text{O}$ , selective deuteration at the  $\text{C}_\alpha$  of the alcohols was observed due to a rapid  $\text{Ru-H}/\text{D}^+$  exchange, which was also deduced theoretically. This process involves a reversal of polarity of the  $\text{D}^+$  ion, which is transformed into a  $\text{Ru-D}$  function ("umpolung"). Negligible deuterium labeling was observed for the imine, possibly due to the high activity in the TH process and also to the decrease in the hydrido complex concentration due to the stability of a hydrido-imine intermediate. Both facts should ensure that the TH reaction will compete favorably with the  $\text{Ru-H}/\text{D}^+$  exchange. The basic nature of the imine hydrogenation product can also hinder the stated  $\text{Ru-H}/\text{D}^+$  exchange. On the basis of DFT calculations, all these hypotheses are discussed. In addition, calculations at this level also support the participation of the stated aqua, formato, and hydrido intermediates in the catalytic reaction and provide a detailed microscopic description of the full catalytic cycle. In the case of the imine TH process, the formation of the hydrido complex (decarboxylation step) is clearly the limiting step of the cycle. On the contrary, in the hydrogenation of cyclohexanone, both decarboxylation and reduction steps exhibit similar barriers, and due to the limitations of the solvent model employed, a definitive conclusion on the rate-determining step cannot be inferred.

**KEYWORDS:** hydrogen transfer, deuterium labeling, ruthenium, density functional calculations, umpolung, catalysis in water



## INTRODUCTION

Labeling with deuterium is a useful procedure to obtain molecules and biomolecules with a wide range of applications.<sup>1</sup> Deuterium-labeled molecules can be used, for instance, as solvents in NMR spectroscopy, labeled drugs, probes in mass spectrometry, probes for mechanistic studies in chemical and biochemical processes, and as raw materials for other labeled compounds and polymers. As a consequence, increasing interest in chemical research has been focused on the development of methodologies for the selective preparation of deuterium-labeled compounds.<sup>1a,2,3</sup> Furthermore, research in deuterium labeling

provides chemical knowledge for tritium labeling, because the chemical procedures developed for deuterium-labeled derivatives can be directly extrapolated to the preparation of the analogous tritium homologues. Labeling with radioisotopes, tritium among them, is a field of great interest that affords an array of applications and plays an important role in the

**Received:** December 21, 2013

**Revised:** February 14, 2014

availability of radiotracers in chemistry, biology, agriculture, and medicine.<sup>4</sup>

$\alpha$ -Deuterated alcohols can be obtained by reduction of the corresponding aldehydes or ketones in stoichiometric reactions with reagents such as NaBD<sub>4</sub>,<sup>5</sup> LiAlD<sub>4</sub>,<sup>6</sup> SiDMe<sub>2</sub>Ph<sup>7</sup> and D<sub>2</sub>/Raney Al.<sup>8</sup> Catalytic procedures introduce time efficiency and economical sustainability in processes to obtain  $\alpha$ -deuterated alcohols that may involve either a reduction or a CH/D exchange between alcohols and an appropriate deuterium source. For example, deuterium-labeled alcohols at the  $\alpha$ - and  $\beta$ -carbon positions have been obtained by H/D exchange reactions between alcohols and C<sub>6</sub>D<sub>6</sub> at 135 °C catalyzed by [Cp\*Ir-(H)<sub>3</sub>(PMe<sub>3</sub>)](OTf) (5 mol %).<sup>9</sup> However, the price of the deuterium source and the harsh experimental conditions are not favorable in this example, and these factors must be considered in the development of future deuterium labeling procedures. D<sub>2</sub>O is the cheapest source of deuterium, and it is also a benign reaction medium. Several CH/D exchange procedures have been carried out using D<sub>2</sub>O and alcohols as starting materials.<sup>10</sup>

As stated above, the reduction of ketones or aldehydes is another alternative for the synthesis of deuterium-labeled alcohols. This method can also be applied to the reduction of imines to give labeled amines.<sup>11</sup> Among the catalytic routes to obtain labeled alcohols and amines, the reduction of ketones and imines by catalytic transfer hydrogenation (TH) offers great potential when the current development of these catalytic procedures is considered. Effectively, TH has been established as one of the most useful methods to achieve the synthesis of alcohols and amines, mainly because it avoids the drawbacks associated with the use of high-pressure molecular hydrogen.<sup>12</sup> 2-Propanol is the preferred hydrogen source in most cases, and Ru-, Rh-, or Ir-based complexes are the most efficient catalytic precursors.<sup>13</sup> Moreover, in selected examples, the reaction can be carried out in water, generally using a mixture of HCOONa and HCOOH as the hydrogen source.<sup>13g,14</sup> Obvious advantages result from the use of water as solvent in that it avoids environmental issues related to the use of organic solvents and it also makes the separation of organic products easier.<sup>15</sup> In contrast, despite the progress made in the transfer hydrogenation of ketones in water, work on the transfer hydrogenation of imines in aqueous media has been scarce to date.<sup>16</sup> Furthermore, applications of TH methods to the preparation of deuterium-labeled alcohols or amines using cheap deuterium sources such as D<sub>2</sub>O have rarely been reported in the literature. To the best of our knowledge, only the studies by Himeda<sup>17,18</sup> can be cited, in which water-soluble complexes, mainly of Ir, were used as catalysts. The degree of deuterium incorporation was variable and fell in the range of 73–92%. For example, in the case of cyclohexanone, 74% deuteration in the  $\alpha$ -position of the alcohol was achieved in the aforementioned work. Moreover, Sajiki also reported the deuterium labeling of alcohols by the reduction of ketones in D<sub>2</sub>O, although these examples involve the use of heterogeneous systems, such as Pd/C<sup>10i,k</sup> or Ru/C,<sup>10j</sup> as catalysts.

Species of the general formula  $[(\eta^6\text{-arene})\text{RuCl}(\text{N,N})]^+$ , where N,N is a diamine or aminoamido ligand, show good activities in both conventional<sup>19</sup> and asymmetric<sup>20</sup> transfer hydrogenation catalysis in water provided that they are soluble in this medium. The pioneering work by Himeda,<sup>17</sup> using [Cp\*M(H<sub>2</sub>O)(bpy)]<sup>2+</sup> (M = Rh, Ir; bpy' = 4,4'-dihydroxy-2,2'-bipyridine) and Ogo et al., using [Cp\*Ir(H<sub>2</sub>O)<sub>3</sub>]<sup>2+</sup> complexes as precatalysts,<sup>21</sup> on the hydrogenation of ketones in water have inspired subsequent studies in which our group and others have exploited the activity of chlorido and aqua complexes

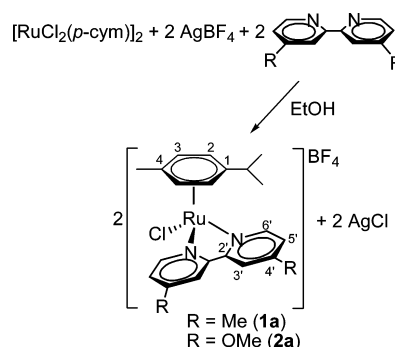
of general formula  $[(\eta^6\text{-arene})\text{Ru}(\text{N,N})(\text{X})]^{n+}$  (X = Cl, H<sub>2</sub>O; n = 1, 2), where N,N in this case is a bipyridine- or phenanthroline-derived ligand.<sup>22,23</sup>

Herein, we describe our complexes  $[(\eta^6\text{-}p\text{-cym})\text{RuCl}(\text{dxbpy})](\text{BF}_4)$  ( $p\text{-cym}$  =  $p$ -cymene; dxbpy = 2,2'-bpy derivatives), which are not only active catalysts in the transfer hydrogenation of several ketones in neat water using formate/formic acid as the hydrogen source but also active toward one imine. Excellent recycling properties have been demonstrated for these water-soluble derivatives, which seem to be more resistant to changes in pH than similar catalytic systems reported previously.<sup>21a,23c</sup> Moreover, one of the most important contributions of this work is the demonstration that these precatalysts are capable of conjugating the hydrogen transfer processes of ketones with a good to high regioselective deuterium labeling of the resulting alcohols in the CDOH  $\alpha$ -position, using only deuterated water as the deuterium source. The present experimental work is accompanied by detailed DFT studies that are congruent with the existence of a reversible and rapid deuteration of the active catalytic hydrido species  $[(\eta^6\text{-}p\text{-cym})\text{RuH}(\text{dxbpy})]^+$ , a process that is coupled to the hydrogenation catalytic cycle. This process allows an effective hydride/deuteron exchange that is the origin of the selective incorporation of deuterium in the  $\alpha$ -position of the alcohol. This step occurs through the reversal of the polarity of the D<sup>+</sup> ion, which is transformed into a deuteride Ru–D function. The German term “umpolung” has been coined for this type of reactivity.<sup>18,24</sup>

## RESULTS AND DISCUSSION

**Synthesis and Structural Characterization of 1a.** The new compound  $[(\eta^6\text{-}p\text{-cym})\text{RuCl}(\kappa^2\text{-}N,N\text{-dmbpy})](\text{BF}_4)$  (**1a**) was synthesized by abstraction of the chloride ligand of the starting ruthenium  $p$ -cymene dimer with AgBF<sub>4</sub> and reaction with the commercially available ligand 4,4'-dimethyl-2,2'-bipyridine (dmbpy) (see Scheme 1). The complex  $[(\eta^6\text{-}p\text{-}$

**Scheme 1. Synthesis Procedure and Numbering Scheme for 1a and 2a**



$\text{cym})\text{RuCl}(\kappa^2\text{-}N,N\text{-dmbpy})](\text{BF}_4)$  (dmbpy = 4,4'-dimethoxy-2,2'-bipyridine) (**2a**), previously reported by our research group,<sup>22</sup> was synthesized for the sake of comparison.

The ruthenium complexes were obtained in moderate to good yields (80 and 64% for complexes **1a** and **2a**, respectively) as air- and moisture-stable yellow solids. The complexes are water-soluble in the concentrations of the catalytic reactions described in this work (10.5 and 2.9 mg·mL<sup>-1</sup> for **1a** and **2a**, respectively).

The new complex **1a** was fully characterized by elemental analysis, FAB<sup>+</sup> mass spectrometry, molar conductivity, and IR

and also by  $^1\text{H}$ ,  $^{19}\text{F}\{^1\text{H}\}$  and  $^{13}\text{C}\{^1\text{H}\}$  NMR spectroscopy and single-crystal X-ray diffraction (see SI for discussion of this X-ray structure). Full assignment of the resonances in the  $^1\text{H}$  and  $^{13}\text{C}\{^1\text{H}\}$  NMR spectra was performed using 2D NMR correlation experiments such as gCOSY, NOESY, and gHSQC.

The  $^1\text{H}$  NMR spectrum of complex **1a** in  $\text{CD}_3\text{OD}$  showed a  $\text{C}_s$  symmetry pattern. Only two mutually coupled signals were observed for the aromatic protons of the *p*-cymene ring and the methyl protons of the *i*Pr group were equivalent. Furthermore, only three signals were observed for the bipyridine rings and one signal for the methyl substituents. On the other hand, as previously observed for the dmbpy derivative **2a**, the dmbpy ligand signals were shifted downfield with respect to those of the free ligand, and this is a consequence of coordination to the metallic center.<sup>25</sup> As expected,  $\delta(\text{H}^{6'})$  is particularly sensitive to this effect due to its proximity to the N-coordinated atom ( $\Delta\delta(\text{H}^{6'}) = 0.8$  ppm).

The  $^{13}\text{C}\{^1\text{H}\}$  NMR spectra show characteristic signals for the dmbpy and the *p*-cymene ligands, with symmetry patterns fully consistent with those shown by  $^1\text{H}$  NMR (see the Experimental Section). The presence of the  $\text{BF}_4^-$  anion was corroborated by the existence of two singlets in the  $^{19}\text{F}\{^1\text{H}\}$  NMR spectrum at  $-154.77$  and  $-154.82$  ppm in a 1:4 ratio ( $^{10}\text{B}/^{11}\text{B}$ ).

The  $\text{FAB}^+$  spectrometry and the conductimetry are compatible with the molar mass and monocationic nature of **1a** (see the Experimental Section). The FT-IR spectrum shows the expected values for the vibration modes of the Ru–Cl group and the  $\text{BF}_4^-$  counteranion.

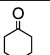
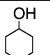
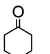
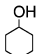
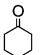
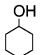
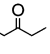
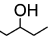
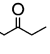
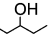
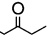
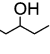
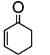
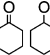
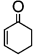
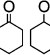
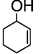
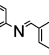
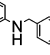
**Catalytic Transfer Hydrogenation of Ketones and Imines in Water.** In order to gain information for our isotopic labeling studies, we decided to test previously the activity of our complexes in the catalytic transfer hydrogenation in neat water with three different ketones (cyclohexanone, 3-pentanone, and 2-cyclohexenone) and one imine (*N*-benzylideneaniline). A mixture of sodium formate/formic acid (pH = 4.4) as the hydrogen source under a nitrogen atmosphere was used, according to the conditions established in the bibliography for similar complexes.<sup>22,23,26</sup> More detailed reaction conditions and the main results are collected in Table 1 (see the Experimental Section for more experimental details and the Supporting Information for additional catalytic results).

The ketones used in these experiments and the resulting alcohols are soluble in water under the experimental conditions at room temperature, and thus the estimated yields can be calculated by direct analysis of the final solutions by  $^1\text{H}$  NMR. This is not the case for *N*-benzylideneaniline and the resulting amine, both of which are insoluble in water at room temperature. As a consequence, the yield was calculated after the extraction of the reaction mixture with diethyl ether and subsequent evaporation of the solvent.

The three different ketones used were extensively reduced under the experimental conditions. On using precatalyst **2a**, the yield of cyclohexanol was only slightly higher than with precatalyst **1a** (entries 1 and 2), and similar results were obtained in the hydrogenation of 3-pentanone (entries 4 and 5). Thus, it can be concluded that both precatalysts show similar behavior. For this reason, only the new precatalyst **1a** was used for the rest of the study reported here.

The straight-chain ketone, 3-pentanone, is converted to the corresponding alcohol less efficiently than the cyclic ketone, cyclohexanone (compare entries 3 and 6), possibly due to steric reasons, as observed previously for precatalyst **2a**.<sup>22</sup> This type of behavior is not uncommon in transfer hydrogenation. For

**Table 1. Catalytic Transfer Hydrogenation Results for Different Substrates Using **1a** or **2a** under Different Reaction Conditions<sup>a</sup>**

Entry	Precat.	Subst.	Prod.	Time	Yield <sup>b</sup>	TON <sup>c</sup>	TOF <sup>d</sup>
1	<b>2a</b>			7	>99	200	28
2	<b>1a</b>			7	91	182	26
3	<b>1a</b>			10	>99	200	20
4	<b>2a</b>			7	62	124	18
5	<b>1a</b>			7	62	124	18
6	<b>1a</b>			24	96	192	8
7	<b>1a</b>			7	95/5		
8	<b>1a</b>			24	0/>99		
9	<b>1a</b>		–	7	0	–	–
10	<b>1a</b>			2	81	162	81

<sup>a</sup>Experiments were repeated at least twice to corroborate reproducibility.  $T = 85^\circ\text{C}$ , cat/S/ $\text{HCOONa} = 1/200/6000$ , [cat] = 0.32 mM, 2 mL  $\text{H}_2\text{O}$ , pH = 4.4 adjusted with  $\text{HCOOH}$ . <sup>b</sup>Yields calculated from  $^1\text{H}$  NMR integrations. <sup>c</sup>TON: mol of product/mol of precatalyst. <sup>d</sup>TOF: mol of product/mol of precatalyst  $\times$  h (calculated at the end of the reaction).

instance, when  $[\text{RuH}(\text{L})(\text{PPh}_3)_2]\text{Cl}$  ( $\text{L} = 2,6\text{-bis}(1,5\text{-diphenyl-1H-pyrazol-3-yl})\text{pyridine}$ ) was used as the precatalyst for the transfer hydrogenation of ketones in 2-propanol under reflux, the activity followed the trend: cyclopentanone  $\gg$  cyclohexanone  $>$  2-heptanone  $>$  3-heptanone.<sup>27</sup>

The reduction of 2-cyclohexenone proceeded efficiently and two products, cyclohexanone and cyclohexanol, were detected during the reaction, meaning that both the alkene and carbonyl functions are reduced under these conditions (entries 7 and 8). The reaction is highly chemoselective for the hydrogenation of the  $\text{C}=\text{C}$  double bond that is reduced first, and only when the conversion to cyclohexanone is almost complete does cyclohexanol begin to appear in the reaction medium (Figure 1). In fact, the formation of 2-cyclohexenol was not observed. This chemoselectivity is commonly observed for the transfer hydrogenation of  $\alpha,\beta$ -unsaturated ketones.<sup>28</sup> In the first step, 2-cyclohexenone is reduced to cyclohexanone with a slightly better yield than the transformation of cyclohexanone into cyclohexanol (compare entries 2 and 7). In a different experiment, it was observed that 2-cyclohexenol was not reduced at all in identical conditions (entry 9). This suggests that the mechanism of the first hydrogenation of 2-cyclohexenone to cyclohexanone involves the participation of the keto group. The mechanism for the selective formation of cyclohexanone from 2-cyclohexenone probably involves a 1,4-reduction of the substrate through a keto–enol tautomerization, as suggested for the transfer hydrogenation of comparable substrates<sup>29</sup> (see Scheme 2).

The activity for the hydrogenation of the imine benzylideneaniline (entry 10) was much higher than for ketones. Yield of the



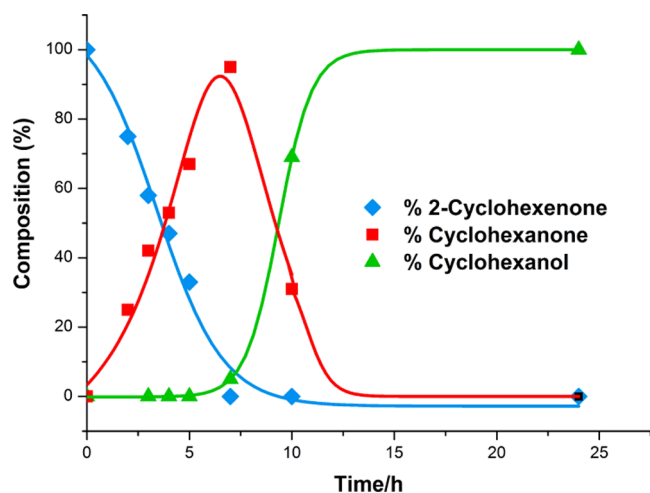
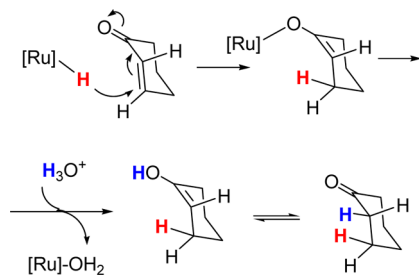


**Figure 1.** Evolution vs time of the ratio of different species for the TH of 2-cyclohexenone using **1a** as precatalyst in neat water.

**Scheme 2. Proposed Hydrogen Transfer Mechanism for the Chemoselective Reduction of 2-Cyclohexenone**



amine was 81% after 2 h of reaction, whereas only 20–30% was achieved in this time on using ketones as substrates, with 5–10 h required to reach a similar yield. The conversion of the imine at 7 h was 90%. Reduction of imines to amines is a rare process in water, and very few examples of such a reaction have been described in the literature.<sup>16,30,31</sup>

**Kinetic Measurements.** In an effort to gain an insight into the values of the initial rate constants and kinetic parameters for the transfer hydrogenation processes described above, the decay with time of selected resonances of the cyclohexanone and 2-cyclohexenone substrates was followed by <sup>1</sup>H NMR experiments under isothermal conditions in H<sub>2</sub>O or D<sub>2</sub>O. The integration of the resonances of substrate and product in each experiment was used. Details of the experiments can be found in the Supporting Information. An induction period was not observed in the conversion versus time plots, and ketone reduction was observed immediately after thermal equilibration of the reaction mixture. Experimental conditions in the NMR tubes were adjusted to be identical to those mentioned above for catalytic experiments, except that stirring was achieved by the sample spinning in the NMR machine (20 Hz) rather than by magnetic stirring. A plot of Ln[substrate] versus time gave a linear fit that is representative of a pseudo-first-order kinetic behavior, with the slope of the line corresponding to a first-order rate constant  $k$  (s<sup>−1</sup>) (see Table S10 and representation in the Supporting Information).

The rate constants for the reduction of cyclohexanone at different temperatures were calculated (entries 1–4 in Table S10). Considering the Eyring theory, activation parameters were calculated, and the following values were obtained:  $\Delta H^\ddagger = 22 \pm 5$  kcal mol<sup>−1</sup> and  $\Delta S^\ddagger = -16.3$  e.u. These values are consistent with

those found in comparable processes<sup>32</sup> and with the energy barrier of the limiting step of our calculations (see below).

**Catalyst Recycling.** Despite the current interest focused in the use of complexes similar to **1a** in catalytic TH processes of ketones in neat water, to the best of our knowledge, studies concerning the recyclability of the catalysts in these processes have not been reported until now. The recycling of the catalyst (precatalyst **1a**) was assessed for the hydrogenation of cyclohexanone. Cycles of 20 h of reaction were applied to ensure complete transformation of the substrate. After each cycle, the product was extracted with diethyl ether under an inert atmosphere (see the Experimental Section for details), and fresh substrate was added to the reaction medium without new addition of either sodium formate, formic acid, or catalyst. The activity of the catalyst without addition of the acid is remarkable, because pH dependence of the catalytic activity has been concluded in previous studies.<sup>21c,23</sup> The activity is also noteworthy bearing in mind that at the beginning of the first step, the ratio formic acid/cyclohexanone is only 5/1 in a process where protons are consumed in the formation of the alcohol and where the successive extractions with diethyl ether could decrease this ratio even more. Four cycles were run, and the yield was above 99% for each one. At the end of the fourth cycle, the pH of the aqueous phase was 9.1. This fact indicates that the formic acid has been consumed or extracted during the reaction and that the hydrogenation has been produced at even higher pH than the initial and optimal value (pH = 4.4). This experiment demonstrates the excellent behavior of the catalyst in the recycling protocol and also proves that, over long reaction times, the activity of **1a** is preserved over a broad range of pH values.

**Formation of Catalytic Intermediates from 1a in Water Solution and Detection of a RuH–D<sup>+</sup> exchange.** In order to obtain information about the mechanism of the transfer hydrogenation process and to detect possible intermediates or active species, we studied the stability of complex **1a** in aqueous solution by <sup>1</sup>H NMR spectroscopy and also evaluated the effect of the addition of HCOONa to the solution.

First, as reported for similar [Ru(arene)Cl(N,N)]<sup>+</sup> compounds in D<sub>2</sub>O solution at pH = 7, the <sup>1</sup>H NMR spectrum of complex **1a** reveals the existence at room temperature of an equilibrium between the chlorido species **1a** and the aqua complex [( $\eta^6$ -*p*-cym)Ru(OD<sub>2</sub>)( $\kappa^2$ -*N,N*-dmbpy)]<sup>2+</sup> (**1b**) with a chlorido/aqua-complex integration ratio of 58:42 (Figure 2a).<sup>22,23d,33</sup> Afterward, an excess of NaCOOH (NaCOOH/cat = 3.5/1) was added to this solution at pH 7. A new set of signals, corresponding to the formate complex [( $\eta^6$ -*p*-cym)Ru(OCOH)( $\kappa^2$ -*N,N*-dmbpy)]<sup>+</sup> (**1c**), was observed after several minutes, and the aqua complex signals decreased (see Figure 2b). The most characteristic resonance for this compound is a singlet at 7.8 ppm, which is assigned to the coordinated formate ligand. Finally, after 10 h, a new set of signals appeared due to a different complex (Figure 2c). These signals are assigned to the hydrido derivative [( $\eta^6$ -*p*-cym)RuH( $\kappa^2$ -*N,N*-dmbpy)]<sup>+</sup> (**1d**).

The signals of the hydrido derivative were shifted upfield relative to those of the other species, which is consistent with the literature examples for similar systems.<sup>23c–e,34</sup> Interestingly, the Ru–H resonance was not detected at low frequencies. A rapid Ru–H/Ru–D exchange in the D<sub>2</sub>O medium could be the reason for the absence of this signal. In order to demonstrate this hypothesis, this last experiment was carried out again in H<sub>2</sub>O. In this experiment, similar NMR resonances were observed, but in this case, they appeared together with the corresponding hydride signal at −6.30 ppm with an integration that was consistent with

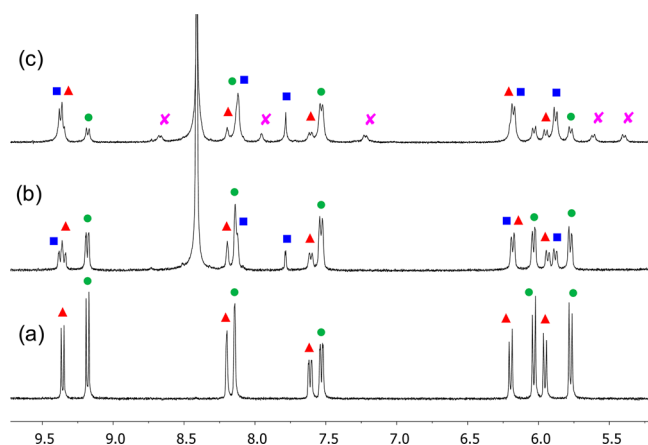


**Figure 2.** (a)  $^1\text{H}$  NMR spectrum of complex **1a** in equilibrium with the aqua-complex **1b**, in  $\text{D}_2\text{O}$  at room temperature. (b) Initial sample evolution after the addition of excess  $\text{HCOONa}$ . (c) Sample evolution after 10 h. Symbols: (red triangle) aqua-complex **1b**, (green circle) chlorido-complex **1a**, (blue square) formato-complex **1c**, and (pink X) hydrido-complex **1d**.

the rest of resonances of this derivative. The ratio of the different species at room temperature (chlorido/aqua/formato/hydrido derivatives) after 10 h was 45:19:19:17. When the temperature was increased to  $70^\circ\text{C}$ , this ratio changed significantly to 45:10:7:38, with an increase in the amount of the hydrido complex at the expense of the aqua and formato derivatives. The reactivity sequence of chlorido–aqua–formato–hydrido complexes is deduced from these experiments. This sequence probably occurs in the catalytic cycle for transfer hydrogenation previously to the reaction with the substrate.

**Deuterium Labeling.** The ready formation of the Ru–D group when  $\text{D}_2\text{O}$  is used as solvent opened the possibility of deuterium labeling of the products obtained from the TH of the different substrates used previously. Accordingly, having optimized the experimental conditions for the hydrogenation processes, the transfer deuteration reactions were carried out with the precatalyst **1a** in  $\text{D}_2\text{O}$  at  $85^\circ\text{C}$  for 24 h to ensure complete transformation of the corresponding substrates. The reaction products were analyzed by  $^1\text{H}$  NMR spectroscopy in order to quantify yields and deuterium incorporation in the different chemical positions. Considering the percentage of deuterium in the solvent and the incorporation of protium in the medium owing to the addition of nondeuterated formic acid, the maximum deuterium incorporation was calculated to be 99.2%.  $^{13}\text{C}\{^1\text{H}\}$  NMR spectroscopy and EI mass spectrometry were used to provide complementary information concerning the deuterium incorporation in the products (see SI). The main results are collected in Table 2.

The  $^1\text{H}$  NMR spectra showed signals for the corresponding alcohol products with an extremely low integration for the  $\text{CH}_\alpha$  group of the alcohol. This fact is due to the deuteration of this position in a ratio that varies from 89 to 97% depending on the substrate and the reaction conditions.

Incorporation of deuterium in the carbon contiguous to the alcohol function ( $\text{C}_\beta$  position) was also observed for cyclohexanol. Deuteration in this position is unexpected for a hydrogen transfer process, but it can be explained by considering the keto–enol tautomerism in the starting ketone, a process that is favored in the acidic medium. This fact was corroborated by following the evolution of cyclohexanone in the reaction medium at  $85^\circ\text{C}$  without the addition of the catalyst. This reaction

**Table 2.** Catalytic Transfer Deuteration Results for Different Substrates Using **1a** under Different Reaction Conditions.<sup>a</sup>

Entry	T ( $^\circ\text{C}$ )	Substrate	Product	D( $\text{C}_\alpha$ )	D( $\text{C}_\beta$ )	D( $\text{C}_\gamma$ )	Time (h)	Yield <sup>b</sup>
1	100			97	26	0	24	>99
2	85	"	"	97	30	0	24	>99
3	75	"	"	93	31	0	24	>99
4 <sup>c</sup>	85	"	"	84	15	0	24	95
5	85		"	89	61	21	24	>99
6	85			94	≅ 3	0	48	91
7	85			0	---	---	24	>99

<sup>a</sup>Experiments were repeated at least twice to corroborate reproducibility. Unless otherwise indicated the conditions used are: cat/S/ $\text{HCOONa}$  = 1/200/6000, [cat] = 0.32 mM, 2 mL  $\text{D}_2\text{O}$ , pD = 4.8 adjusted with  $\text{HCOOH}$ .<sup>35</sup> <sup>b</sup>Yields calculated by  $^1\text{H}$  NMR integrations. <sup>c</sup>pD = 5.6 adjusted with  $\text{HCOOH}$ .

yielded deuterium incorporation in the  $\text{C}_\beta$  position of 28% after 2 h and 34% after 4 h, which are very similar values to those obtained in the alcohol when the hydrogenation process was carried out (30%, entry 2). As expected, deuteration was not observed in the  $\text{C}_{\gamma-\delta}$  positions. The effect of temperature on the deuteration process was studied with cyclohexanone (entries 1–3). Although a very small effect was observed, it seems that an increase in the temperature leads to a higher deuterium ratio in the  $\text{C}_\alpha$  position and to a slight decrease in  $\text{C}_\beta$ .

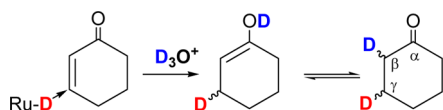
In order to minimize the keto–enol tautomerism, the reaction without catalyst was carried out at higher pH by using only one equivalent of formic acid with respect to cyclohexanone (pD = 5.6) and keeping the rest of parameters constant. The keto–enol tautomerism decreased under these conditions (8% and 16% D( $\text{C}_\beta$ ) in 2 and 4 h, respectively).

When the catalyst was present (entry 4), the increase in pD also led to a decrease in the keto–enol tautomerism (15% D( $\text{C}_\beta$ ) after 24 h). Unfortunately, the deuteration in the  $\text{C}_\alpha$  position also decreased to 84%.

For the reaction with 3-pentanone (entry 6), the keto–enol tautomerism only occurred to a very small extent (approximately 3% D( $\text{C}_\beta$ )), and a high degree of deuterium incorporation in  $\text{C}_\alpha$  was observed (94%). Jia<sup>101</sup> found that the incorporation of deuterium in the  $\beta$ -position is dependent on the acidity of the corresponding C–H bond. In our case, 3-pentanone ( $\text{pK}_\text{a}$  = 27.1) is less acidic than cyclohexanone ( $\text{pK}_\text{a}$  = 26.4) (both values in DMSO).<sup>36</sup>

The deuteration of 2-cyclohexenone is a more complex process than that discussed above. In the 1,4–hydrogenation mechanism, if the transfer occurs, as expected, mainly from a Ru–D group (and not from a Ru–H fragment) an incorporation of close to 25% in  $\text{C}_\gamma$  of cyclohexanone would take place (see Scheme 3). A deuterium incorporation of 25% in  $\text{C}_\beta$  is also expected due to 1,4–hydrogenation. Besides, the keto–enol tautomerism that can operate both in the 2-cyclohexenone starting material and the cyclohexanone, as the product of the first step, would increase the deuterium content in the  $\text{C}_\beta$  positions. According to these considerations, the experimental

### Scheme 3. Deuterium Labeling of 2-Cyclohexenone in the 1,4-Hydrogenation Step



percentages of deuterium incorporation in the  $C_\beta$  and  $C_\gamma$  positions of the cyclohexanol formed are 61 and 21%, respectively (entry 5).

The case of the imine warrants particular attention (entry 7). Deuterium incorporation in the amine was not evidenced by the  $^1\text{H}$  NMR spectrum. When the reaction was carried out using a larger amount of substrate to obtain the  $^{13}\text{C}\{^1\text{H}\}$  NMR spectrum, a very small set of three lines was observed for  $C_\alpha$  (around 48 ppm) together with a major singlet, indicating that a very small proportion of the substrate is deuterated. The low level of deuterium incorporation could be due to the higher activity of the catalyst for the transfer hydrogenation of this substrate, as mentioned previously, and this could exceed the rate of the H/D exchange. Alternatively or additionally, the amine that is produced in the hydrogenation should have an effect on the pH, thus disrupting the H/D exchange process by capturing deuterons. This would have an adverse effect on the deuteration process. This fact was proved by adding an equivalent of  $\text{Et}_3\text{N}$  (with respect to the substrate) in the transfer hydrogenation of cyclohexanone. In this case, only 48% deuteration in the  $C_\alpha$  position (instead 97%) was achieved. However, the addition of double the amount of formic acid in the transfer deuteration process of the imine was not sufficient to improve the degree of deuterium labeling.

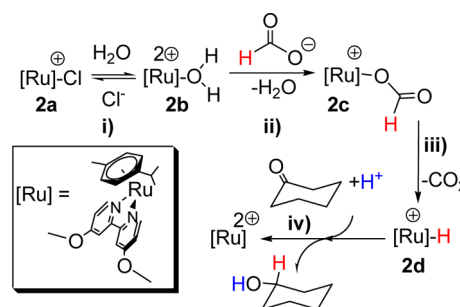
**Ratio of Isotopologues and Isotopomers in the Reaction Products.** With the aim of identifying the formation of different isotopologues and isotopomers, samples of deuterated cyclohexanol and 3-pentanol were analyzed by  $^{13}\text{C}\{^1\text{H}\}$  NMR and also by GC-EI mass for the former. In order not to extend the discussion, only the main conclusions will be presented here. Experimental information and a more detailed discussion can be found in the SI. For all the analyzed samples, the lack of deuterium incorporation in positions beyond  $C_\beta$  of the alcohols was confirmed by  $^{13}\text{C}$  NMR. For a sample of cyclohexanol, a deuterium incorporation of a 92 and a 32%, in positions  $C_\alpha$  and  $C_\beta$ , respectively, was estimated by  $^1\text{H}$  NMR. Due to technical reasons, this sample was previously exchanged with protium in the OH position before it was analyzed by GC-EI mass spectrometry. After this analysis, the determined distribution (%) of isotopologues was  $d_0$  (3%),  $d_1$  (26%),  $d_2$  (37%),  $d_3$  (26%),  $d_4$  (8%),  $d_5$  (<1%). Considering the resonances for  $C_\alpha$  and  $C_\beta$  in the  $^{13}\text{C}$  NMR spectrum, the presence of 6 of the 10 possible isotopomers was determined. In a second sample, obtained in experimental conditions that allowed a more extensive D-incorporation in  $C_\beta$  position, the expected 10 isotopomers were detected.

The  $^{13}\text{C}\{^1\text{H}\}$  NMR spectrum of a sample from the hydrogenation of 3-pentanone was also analyzed, indicating that the major species present in the sample is the molecule  $\text{CH}_3\text{--CH}_2\text{--CDOD--CH}_2\text{--CH}_3$  along with minor amounts of species with  $C_\alpha(\text{H})$  and  $C_\beta(\text{HD})$  groups.

**Computational Study of the Transfer Hydrogenation Mechanism. Mechanistic Considerations and Models.** As stated, complexes **1a** and **2a** have proven to be very effective in the catalytic transfer hydrogenation of ketones and imines with

$\text{HCOOH/HCOONa}$  in aqueous media. NMR studies have shown the sequential participation in the process of aqua, formate, and hydrido intermediates. As previously indicated, related cationic  $\text{Ru(II)}$  arene complexes containing N,N-chelating donor ligands,<sup>23</sup> mainly bipyridines or phenanthrolines, exhibit similar behavior.<sup>23</sup> In several cases, the aqua complex is isolated and used directly as catalyst,<sup>14a,23c</sup> and the hydrido complex is proposed to be the catalytically active species. These systems are unlikely to enable transfer hydrogenation through metal–ligand bifunctional catalysis. Thus, given the pH at which these systems operate (formic acid in the medium), the acidic water medium appears to be the most probable proton source in the reduction process, which is pH dependent. Overall, the experimental evidence is consistent with the following sequence of reactions: (i) chloride by water ligand exchange, (ii) water by formate ligand exchange, (iii) decarboxylation of the formate complex to produce a hydrido species, and (iv) hydride and proton transfer to yield the reduced product (Scheme 4).

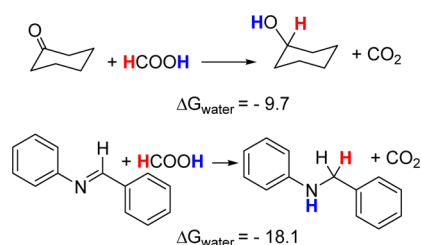
### Scheme 4. Proposed Sequence of Reactions for the Hydrogenation of Cyclohexanone with **2a**



Reactions i–iii lead to the formation of the  $\text{Ru(II)}$  hydrido complex and this should be the species responsible for the hydride transfer in the transfer hydrogenation (reaction iv). In order to obtain a detailed microscopic description and to develop a Gibbs energy landscape of the whole catalytic cycle, we computationally modeled (DFT calculations) all of the proposed steps of the transfer hydrogenation process.

The theoretical study was performed with the chlorido complex **2a** as the catalyst precursor (with no simplifications in the ligands), formate as the hydride source, and both a ketone (cyclohexanone) and one imine (*N*-benzylideneaniline) as the substrates. The thermodynamic viability of both hydrogenations is apparent from the computed Gibbs energies of reaction in water. Reduction of *N*-benzylideneaniline is much more exergonic than that of cyclohexanone (Scheme 5).

### Scheme 5. Calculated Gibbs Reaction Energy in Water ( $\Delta G_{\text{water}}$ , $\text{kcal}\cdot\text{mol}^{-1}$ ) for the Hydrogenation of Cyclohexanone and *N*-Benzylideneaniline with Formic Acid





Recent DFT calculations have highlighted the strong effects that protic solvent molecules, such as water<sup>37</sup> and methanol,<sup>38</sup> can have on proton-transfer reactions in transition-metal-catalyzed reactions. This influence is particularly evident in transfer hydrogenation reactions.<sup>39</sup> In addition, in our system a solvent molecule becomes a ligand. Thus, appropriate solvent modeling is a key issue when computationally studying reaction mechanisms in media in which both specific and nonspecific solute–solvent interactions can be important. A cluster-continuum model, which combines the explicit inclusion of a cluster of solvent molecules with a continuum dielectric medium, appears to be a good methodology to deal with such situations<sup>40</sup> and it has been successfully applied to the study of mechanisms of organometallic reactions in water.<sup>41</sup> In this way, we included three explicit water molecules in the quantum mechanical description of the system in addition to the polarizable continuum model. The effect of the cluster size was assessed by increasing the number of water molecules to five in selected steps. All of the intermediates and transition states were located by full optimization of the complex + substrate + water cluster species into the solvent.

**Formation of the Ru(II) Hydrido Species (From 2a to 2d, Scheme 4).** The catalyst precursor 2a should initially release a chloride ligand. This is a very common and easy process in water. DFT studies have shown that the high Gibbs energy of solvation for the chloride anion in water ( $\Delta G_{\text{sol}}(\text{Cl}^-) = -74.5 \text{ kcal mol}^{-1}$ )<sup>42</sup> is the driving force that favors  $\text{Cl}^-$  dissociation.<sup>41b</sup> However, to the best of our knowledge, a computational study of the reaction has not been published. Using the cluster-continuum model and starting with 2a solvated by three water molecules, we were able to locate the transition state for the chloride by water ligand exchange (TS-Cl-w, Figure 3). In this

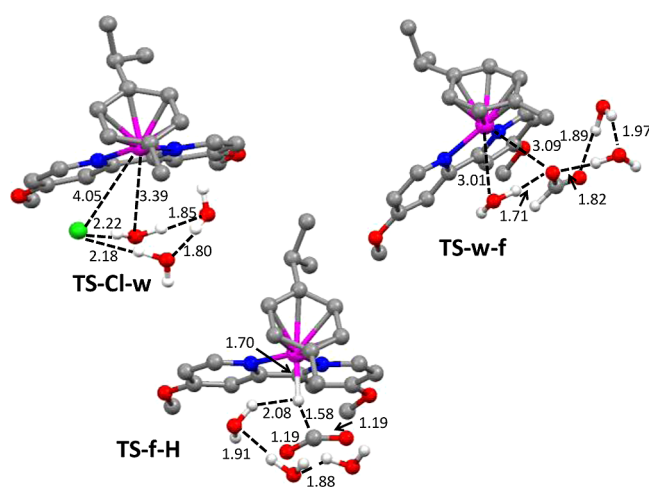


**Figure 3.** Transition states for the chloride–water and water–formate ligand exchanges (TS-Cl-w and TS-w-f, respectively) and the decarboxylation of the formate complex (TS-f-H). Hydrogen atoms in the ligands have been omitted for clarity. Distances are in Å.

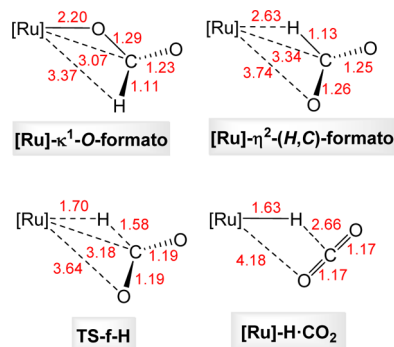
transition state, which is located  $11.1 \text{ kcal mol}^{-1}$  above the solvated 2a, a water molecule initially in the first solvation shell is entering the metal coordination sphere to replace the leaving chloride. This step ends up with a dicationic aqua complex 2b and a chloride anion in the bulk solvent, only  $6.3 \text{ kcal mol}^{-1}$  above 2a. The calculated  $\Delta G_{\text{water}}$  values agree with the ease of the chloride by water ligand exchange in water. Indeed, as stated above, dicationic aqua complexes  $[(\text{arene})\text{Ru}^{\text{II}}(\text{bpy})(\text{H}_2\text{O})]^{2+}$

have been isolated and used as catalytic species for transfer hydrogenation.<sup>14a,23e</sup>

The aqua ligand should be easily displaced by a molecule of the more basic formate ligand. Using our solvent scheme the formate complex 2c is found  $6.6 \text{ kcal mol}^{-1}$  below the aqua complex 2b. Ligand exchange takes place through the transition state TS-w-f (Figure 3), which is only  $2.1 \text{ kcal mol}^{-1}$  above the aqua complex plus a formate anion in the bulk solvent. In the product, the formate adopts a  $\kappa^1\text{-O}$  coordination, and the C–H bond to be broken in the hydride formation step is far away from the metal ( $3.37 \text{ Å}$ ). Therefore, twisting of the formate ligand is required in order to allow the hydrido species to be formed.

$\text{CO}_2$  elimination from the Ru(II) formate complex 2c to generate the hydride and its reverse (i.e., hydride transfer to  $\text{CO}_2$ ) have both been experimentally and theoretically studied in water in related systems with N,N' bidentate ligands.<sup>43</sup> Our results are consistent with previously published results. The  $\kappa^1\text{-O}$ -formate switches to a  $\eta^2\text{-CH}$  metastable intermediate, from which the  $\beta$ -hydride elimination takes place to yield the hydrido complex 2d with the release of  $\text{CO}_2$ . The formate complex evolution along the decarboxylation reaction is represented in Chart 1. The transition state of the  $\text{CO}_2$  elimination (TS-f-H) is

**Chart 1. Calculated Relevant Structures with Selected Geometrical Parameters along the Decarboxylation of the Formate Complex 2c. Distances Are in Å**



depicted in Figure 3. The calculated Gibbs energy barrier from the formate complex 2c is  $14.6 \text{ kcal mol}^{-1}$ . This value is similar, although a bit lower, than the set of barriers that can be found in the literature, which range between  $16.8$  and  $21.7 \text{ kcal mol}^{-1}$  depending on the particular set of ligands.<sup>32,43</sup>

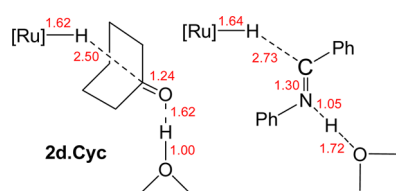
An alternative mechanism has been previously proposed for the activation of the CH bond,<sup>22,23e</sup> involving an arene slippage and the coordination of the formate anion in a quelating  $\kappa^2\text{-O,H-HCO}_2$  way. We have computed a transition state for the decarboxylation step involving an  $\eta^6$  to  $\eta^2$  arene slippage (see Supporting Information). The activation barrier for such a mechanism ( $52.3 \text{ kcal mol}^{-1}$ ) makes it unfeasible.

**C = X Reduction.** The reduction step implies that a hydride and a proton are transferred to the substrate. The hydrido complex 2d is the hydride source, and because transferable protons are not present in the catalyst, thus avoiding the possibility of bifunctional catalysis, the acidic medium should be the proton source. This is the scenario for an ionic hydrogenation mechanism<sup>44</sup> that can be either concerted or stepwise. There is a growing body of evidence that stresses the role that protic solvent molecules can play in transfer hydrogenations of imines and ketones, even when an N–H proton in the ligand makes possible

a concerted bifunctional transfer of two hydrogen atoms through a cyclic transition state.<sup>39b,40,45</sup>

As **2d** (Scheme 4) is a coordinatively saturated complex, the hydride transfer should occur by an outer sphere mechanism.<sup>44</sup> We have optimized an initial outer sphere intermediate for the cyclohexanone reduction, placing a cyclohexanone molecule in the vicinity of complex **2d** and in the presence of a proton solvated by three water molecules. In the resulting optimized intermediate **2d**·cyclohexanone, the C=O bond has the correct orientation to accept the two hydrogen atoms, but the hydride–C and proton–O distances are rather long (2.50 and 1.62 Å, respectively). The ketone is still not protonated at this point (Chart 2).

**Chart 2. Calculated Relevant Structural Parameters in the Initial Intermediates for the TH of Cyclohexanone (Left) and *N*-Benzylideneaniline (Right). Distances Are in Å**



This intermediate leads to the transition state for the hydrogen transfer (TS–HT–keto, Figure 4), and this directly connects

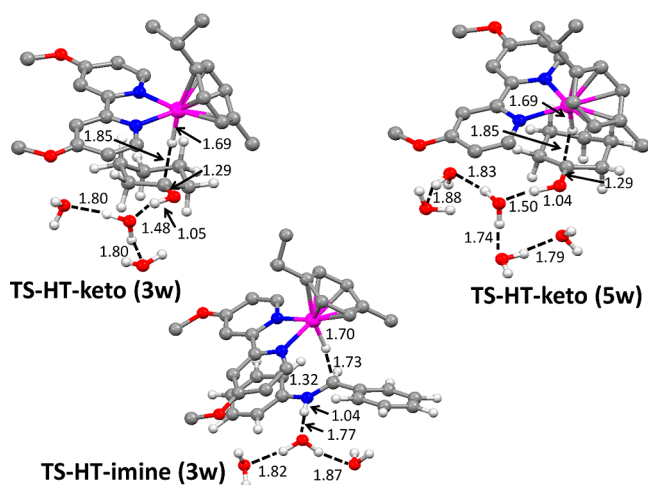


**Figure 4.** Transition states for the hydrogenation of cyclohexanone (three and five water molecules of solvent model, TS–HT–keto (**3w**) and TS–HT–keto (**5w**), respectively) and the hydrogenation of *N*-benzylideneaniline (TS–HT–imine (**3w**)). Hydrogen atoms in the ligands have been omitted for clarity. Distances are in Å.

with the reaction product (cyclohexanol). The process is concerted but is markedly asynchronous; although the proton transfer is already finished in TS–HT–keto ( $O\cdots H = 1.05$  Å), the hydride transfer has only just started ( $C\cdots H = 1.85$  Å). In the reaction product, both the C–H and O–H bonds are fully formed ( $C-H = 1.12$  Å,  $O-H = 0.98$  Å).

The Gibbs energy of activation of the transfer hydrogenation step is very low: TS–HT–keto is located  $8.4 \text{ kcal mol}^{-1}$  above **2d**·cyclohexanone. In order to integrate this value into the catalytic cycle, we must take into account the energy required to generate the proton that is transferred to the substrate in this step. This proton comes from the formic acid; therefore, one must add the

$\Delta G$  of deprotonation of the formic acid in water, which can be easily deduced from its  $pK_a$  (3.75).  $\Delta G_{\text{deprot}}(\text{HCOOH})$  is  $5.1 \text{ kcal mol}^{-1}$ .<sup>46</sup> Addition of this value to  $\Delta G_{\text{HT}}^\ddagger$  ( $8.4 \text{ kcal mol}^{-1}$ ) places the transition state for the HT step  $15.4 \text{ kcal mol}^{-1}$  above **2a**, as can be seen in the Gibbs energy profile depicted in Figure 5.

In an effort to determine whether an improvement in the solvent model could affect our results, we recalculated the barrier of the TH step by adding two more explicit solvent molecules. The transition state TS–HT–keto (**5w**) solvated by five water molecules is shown in Figure 4. This extended network of hydrogen-bonded water molecules leads to a slight increase in the barrier ( $1.4 \text{ kcal mol}^{-1}$ ), but the feasibility of the proposed mechanism is retained.

Wills et al. demonstrated that Ru hydride formation can be the limiting factor in asymmetric transfer hydrogenation catalysis by Ru(II)/ $\eta^6$ -arene-based catalysts with TsDPEN ligands (TsDPEN = *N*-tosyl-1,2-diphenylethane-1,2-diamine).<sup>47</sup> An analogous conclusion is deduced from kinetic studies for the  $\text{CO}_2$  hydrogenation in water by Ogo et al. using a  $[\text{Ru}(\text{arene})\text{-(bipy)}(\text{H}_2\text{O})]^+$  precursor.<sup>48</sup> It can be appreciated in the energy profile (Figure 5) that in our system the barrier for the transfer hydrogenation is considerably lower than that for the  $\text{CO}_2$  elimination in the case of the imine hydrogenation, making the hydride formation from the formate complex the rate-determining step of the process. In contrast, in the ketone hydrogenation, the step of hydride transfer is slightly higher in energy. We must point out that the cluster model suffers from the limitations of the multiple minima corresponding to different water conformations, which can give slightly different energies for the same chemical structure. For this reason, given the small difference between both barriers, we cannot definitively conclude which is the limiting step of the process in this case.

The experimental study has shown that complex **1a** is also active for imine hydrogenation under the same conditions (aqueous solution,  $\text{HCOONa}/\text{HCOOH}$ ). The theoretical study of *N*-benzylideneaniline allows a comparison of the ketone and imine ionic hydrogenation by the same catalytic system. Optimization of the initial complex **2d**·imine in the presence of a proton solvated by three water molecules displays a significant difference in comparison to **2d**·ketone; the imine is already protonated in this initial intermediate (proton–N distance of  $1.05$  Å, Chart 2), which can be described as an iminium cation. This result agrees with recent experimental studies that support an ionic mechanism for imine reduction.<sup>45a,49</sup> The Gibbs energy barrier for the *N*-benzylideneaniline hydrogenation (TS–HT–imine, Figure 5) is  $4.9 \text{ kcal mol}^{-1}$ , which is markedly lower than that for the cyclohexanone reduction ( $8.4 \text{ kcal mol}^{-1}$ ). This finding is consistent with the experimentally measured higher activity for the hydrogenation of the imine than for ketones with complex **1a** (Table 1).

#### Mechanism of the Ru–H/D<sup>+</sup> Exchange in $\text{D}_2\text{O}$ Solution.

Water-soluble phosphine complexes of rhodium(I) and ruthenium(II) catalyze the H/D exchange between  $\text{H}_2$  and  $\text{D}_2\text{O}$  under mild conditions.<sup>14a</sup> Mechanistic studies indicated that the H/D exchange probably involves the deuteration of a hydride species by  $\text{D}_3\text{O}^+$ , resulting in a  $\eta^2$ -HD intermediate that is deprotonated by a solvent molecule (Scheme 6).<sup>50</sup>

In our system, the Ru–D deuteride in the presence of a ketone substrate is selectively incorporated at the  $C_\alpha$  position of the alcohol product. In this process, the deuterium in  $\text{D}_3\text{O}^+$ , polarized as  $O-D(\delta^+)$ , is transferred to a bond polarized as  $\text{Ru}-D(\delta^-)$ , and this allows the deuterium transfer as a



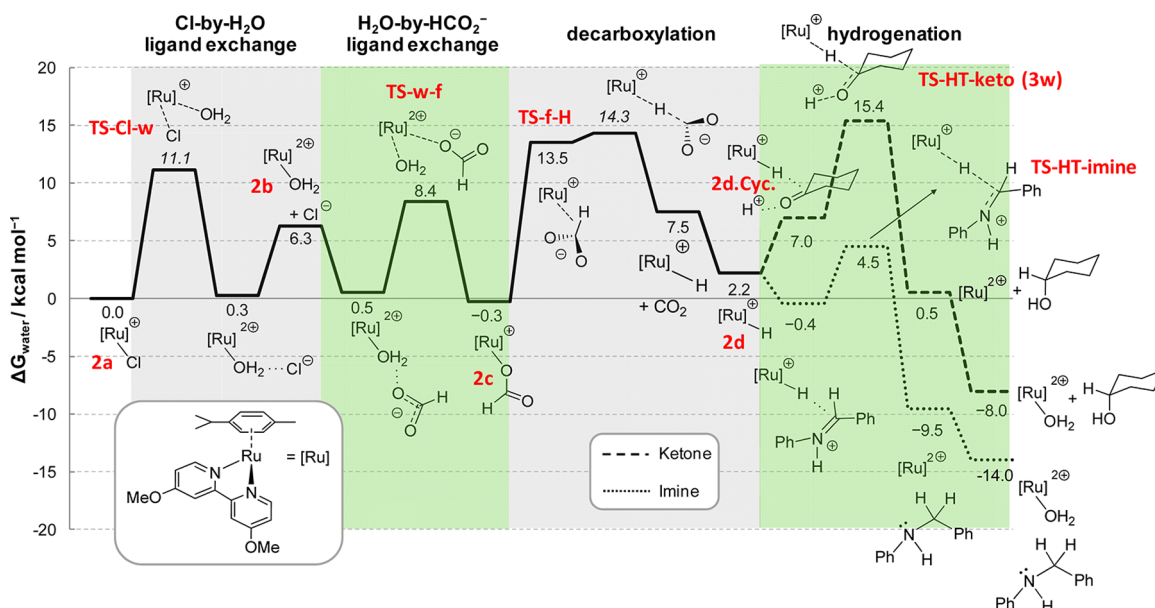
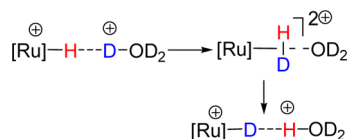


**Figure 5.** Gibbs energy profile in water ( $\text{kcal mol}^{-1}$ ) for the hydrogenation of cyclohexanone (----) and *N*-benzylideneaniline (....). Three explicit water molecules are present in all the calculated structures.  $\Delta G$  of deprotonation of the formic acid ( $5.1 \text{ kcal mol}^{-1}$ ) has been added in the hydrogenation step (see text).

#### Scheme 6. Proposed Mechanism for the Ru–H/ $\text{D}^+$ Exchange in Acidic $\text{D}_2\text{O}$ solution



nucleophilic fragment to  $\text{C}=\text{O}$  functional groups. The term “umpolung” has been coined for this reversal of polarity in a function.<sup>18,24</sup>

We studied theoretically the protonation/deprotonation process of the hydride complex **2d** using our solvent model ( $\text{H}^+$  solvated by three water molecules). As expected, protonation of **2d** is a facile process, which takes place with a Gibbs energy barrier of  $7.6 \text{ kcal mol}^{-1}$  (transition state **TS–H–D**) and leads to a dihydrogen intermediate **2d–H<sub>2</sub>** only  $4.6 \text{ kcal mol}^{-1}$  above the initial hydride. Further deprotonation of the dihydrogen complex by a water molecule (reverse reaction) enables the H/D exchange to occur. The optimized structures of the species involved in the H/D exchange are depicted in Figure 6.

Umpolung of a hydrogen atom is difficult, because the reaction of a deuterium source, such as  $\text{D}_3\text{O}^+$ , with an  $(\text{H}^{\delta-}-\text{M})$  function results in the facile formation of molecular HD, avoiding in this way the deuterium becoming a deuteride anion.<sup>51</sup> This is not the case in our system, which suggests that the dihydrogen intermediate behaves as a strong acid, releasing a proton to the solution and forming the deuteride in a very efficient way. To analyze such a behavior, we estimated the  $\text{pK}_a$  of the coordinated dihydrogen ligand using the theoretical approach that was previously employed for the estimation of  $\text{pK}_a$  values of organometallic complexes.<sup>38d,39a,41b,d</sup> Details of the  $\text{pK}_a$  calculations are provided in the Supporting Information. The calculated  $\text{pK}_a$  of **2d–H<sub>2</sub>** is  $-3.3$ . Although the accurate theoretical calculation of  $\text{pK}_a$  values is still challenging,<sup>52</sup> the value obtained indicates that **2d–H<sub>2</sub>** behaves as a strong acid in water solution, releasing a proton and, in this way, avoiding  $\text{H}_2$

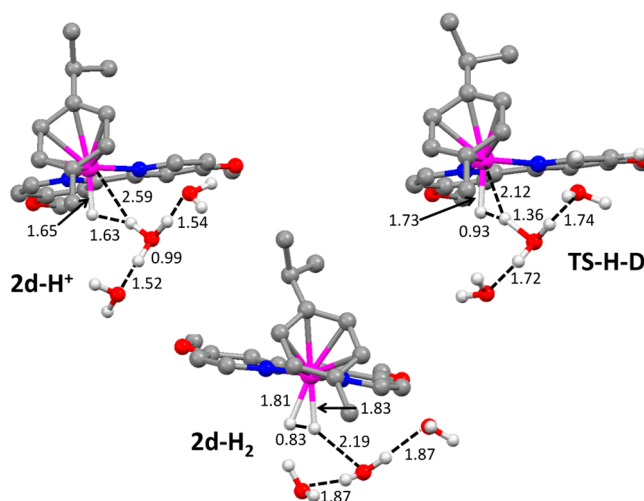
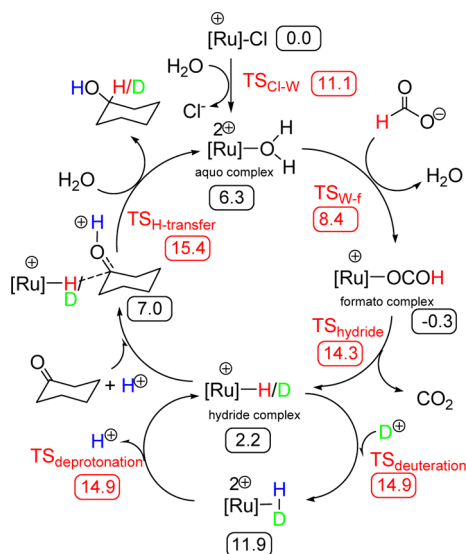


**Figure 6.** Optimized structures of the species involved in the H/D exchange. Hydrogen atoms in the ligands have been omitted for clarity. Distances are in Å.

evolution. Summarizing this acid–base equilibrium in  $\text{D}_2\text{O}$  solution, the Ru–H hydride complex **2d** is a weak base that can be protonated by a strong acid ( $\text{D}^+$ ) to give a strong conjugate acid (dihydrogen complex,  $\text{Ru}(\text{HD})$ ), which in turn transfers a proton to a water molecule. In this way, a metal–hydrido is exchanged with a deuteride, resulting in the umpolung of hydrogen and deuterium atoms.<sup>18</sup> In the presence of a ketone, the coupled transfer hydrogenation allows the subsequent incorporation of the deuteride at the  $\text{C}_\alpha$  position of the alcohol product. A key point in this sequence of reactions is that deuteration ( $\Delta G_{\text{H-D}}^\ddagger = 7.6 \text{ kcal mol}^{-1}$ ) is faster than the hydrogen transfer to cyclohexanone ( $\Delta G_{\text{HT}}^\ddagger = 8.4 \text{ kcal mol}^{-1}$ ). This explains the high degree of deuterium incorporation in the  $\alpha$ -position of the alcohols. The coupled TH/deuteration catalytic cycle for cyclohexanone is represented in Chart 3, together with

the relative Gibbs energy in water of the most important species in the cycle.

**Chart 3. Mechanism of the Coupled TH/Deuteration Catalytic Cycle<sup>a</sup>**



<sup>a</sup>Relative Gibbs energies (kcal·mol<sup>-1</sup>) in water of intermediates (in black) and transition states (in red) are given.  $\Delta G$  of deprotonation of the formic acid (5.1 kcal mol<sup>-1</sup>) has been added in the hydrogenation and in the deuteration steps (see text).

The experimental study has shown that deuterium incorporation does not occur in the imine hydrogenation. Moreover, the addition of Et<sub>3</sub>N in the transfer hydrogenation of cyclohexanone leads to a decrease in the deuteration process. Calculations provide some hints about this behavior. On the one hand, hydrogenation of *N*-benzylideneaniline ( $\Delta G_{\text{HT}}^{\ddagger} = 4.9$  kcal mol<sup>-1</sup>) is faster than deuteration ( $\Delta G_{\text{H-D}}^{\ddagger} = 7.6$  kcal mol<sup>-1</sup>). A complementary reason resides in the stability of the intermediate that is located between **2d** and **TS-HHT-imine**. This intermediate, where the imine is protonated, is more stable than the monohydride **2d** ( $-0.4$  from  $2.2$  kcal mol<sup>-1</sup>, see Figure 5). The stability of this intermediate should imply a low concentration of **2d** in solution slowing down, as a consequence, the RuH/D<sup>+</sup> exchange process. On the other hand, the basic nature of the hydrogenation product (amine) favors deprotonation of the dihydrogen complex by this product over deprotonation by water. We calculated  $\Delta G_{\text{deprot}}$  of **2d**-H<sub>2</sub> by the reduction product of the imine, benzylphenylamine. In accordance with the basicity scale, deprotonation by the benzylphenylamine is favored ( $\Delta G_{\text{deprot}} = -6.7$  kcal mol<sup>-1</sup>) over deprotonation by water ( $\Delta G_{\text{deprot}} = -6.1$  kcal mol<sup>-1</sup>). The process is even more favored with Et<sub>3</sub>N ( $\Delta G_{\text{deprot}} = -16.6$  kcal mol<sup>-1</sup>). Optimization of **2d**-H<sub>2</sub> in the presence of Et<sub>3</sub>N gives the protonated amine without a barrier. It is clear that when a base stronger than water is present in the solution, it can capture the deuterons, thus hindering substrate deuteration.

## CONCLUSIONS

In order to gain information on the activity and selectivity of complex **1a** and, to a lesser extent, **2a** in catalytic TH, we have used as substrates ketones, cyclohexanone, 2-cyclohexenone and 3-pentanone, and the imine *N*-benzylideneaniline in neat water with HCOONa/HCOOH as the hydrogen source. The C=O

position of 2-cyclohexenone is first hydrogenated in a chemoselective process involving a 1,4-mechanism of hydrogenation. According to the data, the following order of hydrogenation activity is observed: *N*-benzylideneaniline > 2-cyclohexenone > cyclohexanone > 3-pentanone. Excellent recycling efficiency were demonstrated in the TH of the cyclohexanone, for which a quantitative conversion is achieved in four cycles of 20 h without the need to adjust the pH at the end of each cycle. <sup>1</sup>H NMR experiments have allowed us to detect the formation of aqua-, formate-, and hydrido-species in the water solution prior to the reaction with the substrate.

DFT calculations, using a cluster-continuum model for the solvent description, unravel the microscopic details of the hydrogenation process and give the Gibbs energy landscape of the catalytic cycle. In water solution, the chlorido-, aqua-, formate-, and hydrido-intermediates have similar Gibbs energies. Barriers connecting these isoergonic minima are rather low. Transfer hydrogenation takes place with a lower barrier by means of a concerted but highly asynchronous outer-sphere ionic mechanism, with the proton coming from the acid water medium. The barrier of the transfer hydrogenation step is much lower for the imine than for the ketone reduction.

In the case of imine, the barrier for the decarboxylation of the formate complex to yield the hydrido complex is considerably higher than that of the reduction step. In the case of ketone, both barriers are similar.

Finally, and very importantly, we have demonstrated that the TH process in water described here can be coupled to a labeling with deuterium in the  $\alpha$ -position of the alcohols obtained from the ketones using D<sub>2</sub>O as the only deuterium source in a variable level of regioselectivity depending on the substrate and the experimental conditions. In this way, labeling levels of up to 97% were achieved in short times. A coupled and very rapid process of RuH/D<sup>+</sup> exchange has been shown to take place by DFT calculations and experimental results. The metal-hydride intermediate is deuterated by D<sub>3</sub>O<sup>+</sup>, resulting in a  $\eta^2$ -HD intermediate that behaves as a strong acid, transferring the proton to a solvent molecule and yielding the Ru-D species that enters into the TH cycle. This exchange involves the reversal of polarity of D<sup>+</sup>, which becomes a nucleophilic deuteride Ru-D that can be transferred onto the C=O functional group. Very few examples of this behavior, which is described by the term umpolung, can be found in the literature. A minor level of deuterium incorporation in the  $\beta$ -position of the alcohol is also observed due to keto-enol tautomerism in the initial ketone. Comparison of the Gibbs energy barriers for deuteration and TH shows that deuteration is faster than hydrogen transfer to cyclohexanone. The experimental study shows that the investigated imine is not deuterium-labeled. Calculations indicate that for *N*-benzylideneaniline the RuH/D<sup>+</sup> exchange is slower than the TH process. These studies also evidence the formation of a hydrido-iminium intermediate that precedes the imine hydrogenation. The stability of this intermediate will decrease the hydrido complex concentration in the reaction media slowing down, as consequence, the Ru-H/D<sup>+</sup> exchange. Moreover, the basic nature of the imine hydrogenation product (benzylphenylamine) means that it is able to capture the deuterons, thus complicating the substrate deuteration.

Work aimed at the optimization of the experimental conditions to obtain a good level of deuterium labeling in amines and the development of new catalysts that could allow asymmetric TH are currently underway in our laboratory.

## EXPERIMENTAL SECTION

**General.** All manipulations were carried out under an atmosphere of dry oxygen-free nitrogen using standard Schlenk techniques. Solvents were distilled from the appropriate drying agents and degassed before use. Elemental analyses were performed with a Thermo Quest FlashEA 1112 microanalyzer and IR spectra on a Shimadzu IRPrestige-21 IR spectrometer equipped with a Pike Technologies ATR. The FAB<sup>+</sup> mass spectrometry measurements were made with a Thermo MAT95XP mass spectrophotometer with magnetic sector. <sup>1</sup>H, <sup>13</sup>C{<sup>1</sup>H}, and <sup>19</sup>F{<sup>1</sup>H} NMR spectra were recorded on Varian Innova 500, Varian Unity 300, and Varian Gemini 400. Chemical shifts (ppm) are relative to TMS (<sup>1</sup>H, <sup>13</sup>C NMR) and to CFCl<sub>3</sub> (<sup>19</sup>F). The atom numbering is reflected in Scheme 1. Coupling constants (*J*) are in Hertz. <sup>1</sup>H–<sup>1</sup>H COSY spectra: standard pulse sequence with an acquisition time of 0.214 s, pulse width of 10 ms, relaxation delay of 1 s, 16 scans, 512 increments. For <sup>1</sup>H–<sup>13</sup>C g–HMBC and g–HMQC spectra, the standard Varian pulse sequences were used (VNMR 6.1 C software). The spectra were acquired using 7996 Hz (<sup>1</sup>H) and 25133.5 Hz (<sup>13</sup>C) widths; 16 transients of 2048 data points were collected for each of the 256 increments. NOESY spectra were acquired using 8000 Hz width, and 16 transients of 2048 data points were collected for each of the 256 increments, with a pulse time of 1 s and mixing time of 1 s. For variable-temperature spectra, the probe temperature (±0.1 K) was controlled by a standard unit calibrated with a methanol reference. In the NMR analysis, s, d, m, and bs denote singlet, doublet, multiplet, and broad signal, respectively. Unless otherwise stated, the <sup>13</sup>C{<sup>1</sup>H} NMR signals are singlets. The starting material [RuCl<sub>2</sub>(*p*-cymene)]<sub>2</sub><sup>53</sup> was prepared according to literature procedures. The ligands dmbpy and dmboppy as well as the different substrates for the catalytic hydrogenation are commercially available and were used as purchased from Aldrich. Complex **2a** was synthesized as reported previously by our research group.<sup>22</sup> For the molar conductivity measurements, the Λ<sub>M</sub> values are given in S·cm<sup>2</sup>·mol<sup>−1</sup> and were obtained at room temperature for 10<sup>−3</sup> M solutions of the corresponding complexes in CH<sub>3</sub>CN, using a CRISON 522 conductimeter equipped with a CRISON 5292 platinum conductivity cell.<sup>54</sup> For mass spectrometry, a GC-EI Varian 3800 GC coupled with a Varian Triple Quad 1200L detector was used. Twenty and 70 eV were tested as power source for the electronic ionization of the sample, and representative changes in the analyzed signals and in the ionization level of the sample were not observed. The experimental conditions for GC were as follows: column factor IV (30 m × 0.25 mm × 0.25 μm). The temperature-programmed ramps in the oven are indicated in Table 3 below. Helium flux: 1 mL/min; injector

Table 3

temp (°C)	°C/min	hold (min)	total (min)
60	0.0	3.0	3.0
100	8.0	1.0	9.0
250	60.0	0.0	11.5

temperature: 200 °C; split: 200; injection volume: 1 μL. Experimental conditions for EI-MS: window of 35–159 um<sup>a</sup>s; transfer line temperature: 250 °C; source temperature: 200 °C.

**Computational Details.** Calculations were performed at the DFT level using the M06 functional<sup>55</sup> including an ultrafine integration grid, as implemented in Gaussian 09.<sup>56</sup> The Ru atom was described using the scalar-relativistic Stuttgart–Dresden SDD pseudopotential and its associated double-ζ basis set,<sup>57</sup> complemented with a set of *f*-polarization functions.<sup>58</sup> The 6-31G(d,p) basis set was used for the H,<sup>59</sup> C, N, O, and Cl atoms.<sup>60</sup> To take into account both nonspecific and specific interactions with the solvent, a mixed continuum/discrete solvent model was used.<sup>40</sup> In this model, in addition to the continuum description of the solvent (SMD continuum model),<sup>61</sup> three explicit water molecules, able to establish hydrogen-bonding interactions with the catalyst and the substrate, have been included. The effect of increasing the number of explicit water molecules has been checked in selected steps. The structures of the reactants, intermediates, transition states, and products were optimized in water solvent (ε = 78.35) using

this cluster-continuum model. Frequency calculations were carried out for all the optimized geometries to characterize the stationary points as either minima or transition states. Intrinsic reaction coordinate (IRC) calculations<sup>62</sup> were computed for the transition states to confirm they connect with the corresponding intermediates. All the energies collected in the text are Gibbs energies in water at 298 K.

**X-ray Crystallography.** Crystals suitable for X-ray diffraction were obtained by slow diffusion of diethylether in an acetone solution of **1a** at −20 °C. A summary of crystal data collection and refinement parameters for all compounds are given in Table S11.

Single crystals of **1a** were mounted on a glass fiber and transferred to a Bruker X8 APEX II CCD diffractometer equipped with a graphite monochromated Mo Kα radiation source (λ = 0.71073 Å). The highly redundant data sets were integrated using SAINT<sup>63</sup> and corrected for Lorentz and polarization effects. The absorption correction was based on fitting a function to the empirical transmission surface as sampled by multiple equivalent measurements with the program SADABS.<sup>64</sup> The software package SHELXTL version 6.10<sup>65</sup> was used for space group determination, structure solution, and refinement by full-matrix least-squares methods based on *F*<sup>2</sup>. All non-hydrogen atoms were refined with anisotropic displacement except those of BF<sub>4</sub><sup>−</sup> anion, which show disorder. This disorder has been modeled in three different positions using geometrical restraints for each model. Hydrogen atoms were placed using a “riding model” and included in the refinement at calculated positions. CCDC-965179 for **1a**, contain the supplementary crystallographic data for this paper. These data can be obtained free of charge from the Cambridge Crystallographic Data Centre via www.ccdc.cam.ac.uk/data\_request/cif.

**Synthesis of [RuCl(*p*-cym)(dmbpy)]BF<sub>4</sub> (**1a**).** To a solution of [RuCl<sub>2</sub>(*p*-cymene)]<sub>2</sub> (100.0 mg, 0.16 mmol) in 30 mL of ethanol, 63.5 mg of AgBF<sub>4</sub> (0.32 mmol) was added, and the reaction mixture was stirred for 2 h at room temperature in the absence of light. The solution was filtered to eliminate the solid AgCl, and the ligand dmbpy was added (60.1 mg, 0.32 mmol). After the solution was stirred overnight, it was evaporated in vacuum to 10 mL, and pentane (30 mL) was added to precipitate the product as a yellow solid. Yield: 140.6 mg, 80%. Anal. Calcd. for C<sub>22</sub>H<sub>26</sub>BClF<sub>4</sub>N<sub>2</sub>Ru: C, 48.77; H, 4.84; N, 5.17. Found: C, 48.24; H, 4.14; N, 4.96. <sup>1</sup>H NMR (CD<sub>3</sub>OD, 500 MHz, 298 K): 1.03 (d, *J* = 7.0 Hz, 6H, Me<sup>ipr</sup>(*p*-cym)), 2.25 (s, 3H, Me<sup>Tol</sup>(*p*-cym)), 2.61 (s, 6H, Me<sup>dmbpy</sup>), 2.61 (bs, 1H, CH<sup>ipr</sup>(*p*-cym)), 5.83 (d, *J* = 5.7 Hz, 2H, H<sup>3</sup>(*p*-cym)), 6.06 (d, *J* = 5.7 Hz, 2H, H<sup>2</sup>(*p*-cym)), 7.58 (d, *J* = 5.4 Hz, 2H, H<sup>5</sup>), 8.35 (s, 2H, H<sup>3'</sup>), 9.26 (d, *J* = 5.5 Hz, 2H, H<sup>6'</sup>) ppm. <sup>13</sup>C{<sup>1</sup>H} NMR (CD<sub>3</sub>OD, 100 MHz, 298 K): 18.95 (Me<sup>Tol</sup>(*p*-cym)), 21.20 (Me<sup>dmbpy</sup>), 22.26 (Me<sup>ipr</sup>(*p*-cym)), 32.33 (CH<sup>ipr</sup>(*p*-cym)), 85.15 (C<sup>3</sup>(*p*-cym)), 87.97 (C<sup>2</sup>(*p*-cym)), 105.38 (C<sup>4</sup>(*p*-cym)), 105.48 (C<sup>1</sup>(*p*-cym)), 125.51 (C<sup>3'</sup>), 129.58 (C<sup>5'</sup>), 154.12 (C<sup>2'</sup>), 155.95 (C<sup>6'</sup>), 155.99 (C<sup>4'</sup>) ppm. <sup>19</sup>F{<sup>1</sup>H} NMR (CD<sub>3</sub>OD, 376 MHz, 298 K): −154.77(s), −154.82(s) ppm, 1/4 ratio. IR: 3082 (ν(C<sub>arom</sub>–H)), 2972 (ν(C<sub>alk</sub>–H)), 1620, 1485 (ν(C=C) + ν(C≡N)), 1051 (ν(B–F)) cm<sup>−1</sup>. MS (FAB<sup>+</sup>, SA): *m/z* (assign., rel int. %): 455 [(M–BF<sub>4</sub>)<sup>+</sup>, 100.0], 420 [(M–BF<sub>4</sub>–Cl)<sup>+</sup>, 10.3], 321 [(M–BF<sub>4</sub>–(*p*-cym))<sup>+</sup>, 6.5]. Molar conductivity value, Λ<sub>M</sub>, in CH<sub>3</sub>CN: 126 S·cm<sup>2</sup>·mol<sup>−1</sup>.

**Catalytic Transfer Hydrogenation.** The NaHCOO/HCOOH buffer solution was prepared from HCOONa (6.53 g, 96.0 mmol) and 650 μL (17.2 mmol) of HCOOH in water (HPLC grade). The volume was adjusted to 25 mL in a volumetric flask. The precatalyst solution was prepared by dissolving 16 μmol of the corresponding catalyst (**1a** or **2a**) in water (HPLC grade) and adjusting the volume in a 25 mL volumetric flask. Once the solutions had been prepared, nitrogen was bubbled through for several minutes, and they were stored under an inert atmosphere.

For the catalytic runs, 1 mL of the buffer solution (HCOONa/HCOOH) and 1 mL of the catalyst solution were added to a 10 mL ampule sealed with a Young valve. The substrate was then added by microsyringe (0.128 mmol of the different substrates: 13.6 μL of 3-pentanone, 13.3 μL of cyclohexanone, 12.5 μL of 2-cyclohexenone, or 23.2 mg of *N*-benzylideneaniline) and nitrogen was bubbled through. The ratio cat/substrate/HCOONa was 0.64 μmol/0.128 mmol/3.84 mmol = 1/200/6000, and the precatalyst concentration was 0.32 mM. For each experiment, two ampules with identical concentrations were



introduced simultaneously in a homemade multihole reactor preheated at 85 °C (mineral oil bath and temperature sensor control), and the mixtures were magnetically stirred for the corresponding reaction time. The ampoules were then cooled in an ice/water bath, and the solutions were transferred to a 5 mL vial and kept refrigerated until analysis. In the case of the reduction of the water-insoluble *N*-benzylideneaniline, the resulting liquor was extracted with diethyl ether (3 × 5 mL). The organic solvent was then evaporated under a stream of dry nitrogen.

Experiments were considered as valuable when a difference <3% was deduced from the liquor of both ampoules.

Analysis of the samples was carried out as follows: The sample (300 μL) was introduced into a 5 mm NMR tube sealed with a concentric capillary and charged with D<sub>2</sub>O. The <sup>1</sup>H NMR spectrum was recorded, and the different resonances of substrates and products were integrated to calculate the corresponding yields. In the case of *N*-benzylideneaniline, the analysis was carried out by dissolving the extracted product in 500 μL of CDCl<sub>3</sub>. The ratio between resonances was evaluated to calculate the yield of the amine. The following resonances were used: 2.56 ppm (4H, C<sup>2</sup>H<sub>2</sub>) for cyclohexanone; 1.70 ppm (1H, C<sup>4</sup>H<sub>2</sub>) for cyclohexanol; 2.78 ppm (C<sup>5</sup>H<sub>2</sub>) for 2-cyclohexenone; 1.34 ppm (Me) for 3-pentanone; 1.21 ppm (Me) for 3-pentanol; 8.39 ppm (1H, CH imine) for *N*-benzylideneaniline; 4.26 ppm (2H, CH<sub>2</sub>) for phenylbenzylamine. In all cases, the residual water signal was considered as a reference (4.63 ppm). No other reaction products were observed in the <sup>1</sup>H NMR spectra.

**Catalyst Recycling.** The study was carried out using cyclohexanone as the substrate. After the first catalytic cycle, carried out as described above at 85 °C for 20 h, the reaction was stopped in an ice/water bath. Once the solution was at room temperature, it was extracted under an inert atmosphere by adding diethyl ether (2 × 5 mL) to the aqueous liquor. For this extraction, the mixture was stirred vigorously for 30 min, left to stand, and decanted. The organic phase was separated with a Pasteur pipet. The organic solvent was then evaporated under a stream of dry nitrogen. The yield was calculated from the <sup>1</sup>H NMR spectrum in CDCl<sub>3</sub>. Fresh cyclohexanone was then added to the aqueous phase and a new cycle was run. A total of four cycles were studied.

**Kinetic Measurements.** For the kinetic measurements, <sup>1</sup>H NMR experiments were carried out in 5 mm NMR tubes. The procedure was similar to that described for the catalytic transfer hydrogenation experiments with the corresponding decrease in the buffer, catalyst, and substrates volumes. For the catalytic runs, 250 μL of the buffer solution (HCOONa/HCOOH) and 250 μL of the catalyst solution were added to a 5 mm NMR tube sealed with a Young valve. The substrate was then added by microsyringe (0.032 mmol of the different substrates: 3.3 μL of 2-cyclohexan-1-one or 3.1 μL of 2-cyclohexen-1-one) and nitrogen was bubbled through. The ratio cat/substrate/HCOONa was 0.16 μmol/0.032 mmol/0.96 mmol = 1/200/6000. The NMR tube was introduced into the probe, previously preheated to the corresponding temperature, and an array of acquisitions was carried out. Each of the NMR spectra of these arrays was integrated, and the integrations of the appropriate resonances were considered for calculations (see SI).

**Selective Deuteration Experiments.** The buffer solution was prepared in D<sub>2</sub>O with 1.306 g of HCOONa (19.2 mmol) and 130 μL of HCOOH (3.44 mmol) in a 5 mL volumetric flask and was stored under an inert atmosphere after bubbling nitrogen through for several minutes. The precatalyst solution was prepared by dissolving 3.2 μmol of the corresponding complex (**1a** or **2a**) in D<sub>2</sub>O and adjusting the volume to 5 mL in a volumetric flask.

The catalytic reaction samples were prepared in Teflon-capped 10 mL Young ampoules under an inert atmosphere with 1 mL of each solution and 0.128 mmol of the different substrates. After bubbling the solutions with N<sub>2</sub>, the ampoules were introduced into a preheated oil bath with the temperature controlled by a sensor controller, and the reaction mixtures were stirred for 24 h. The ratio cat/substrate/HCOONa was 0.64 μmol/0.128 mmol/3.84 mmol = 1/200/6000, and the precatalyst concentration was 0.32 mM. After cooling the mixture in an ice/water bath, 0.5 mL samples were analyzed directly by <sup>1</sup>H NMR spectroscopy.

Samples with 0.70 mmol of substrate (without varying the rest of components) were used to obtain samples with higher deuterium incorporation in the β-position of the alcohol. In these cases, the

reaction mixture was stirred for 3 days to ensure complete transformation of the substrates. Products were extracted with diethyl ether (3 × 5 mL), and the solvent was evaporated under a stream of nitrogen. The <sup>13</sup>C{<sup>1</sup>H} NMR samples were prepared in these cases in CDCl<sub>3</sub>.

**Aqueous Solution Chemistry.** The aquation–anation equilibrium of the Ru<sup>II</sup> chloro complex **1a**, was monitored by <sup>1</sup>H NMR spectroscopy. The spectra were recorded for 18 mM solutions in D<sub>2</sub>O at various time intervals (10, 17, and 24 h), and the signals were referenced to TMS via the residual resonance of water. The relative amounts of the Ru<sup>II</sup> chloro–complex and the aqua derivative were determined by integration of the respective <sup>1</sup>H resonances.

$[(\eta^6\text{-}p\text{-cymene})\text{RuCl}(\text{dmbpy})]^+(\mathbf{1a})$ . <sup>1</sup>H NMR (300 MHz, D<sub>2</sub>O, 298K): δ 1.02 (d, *J* = 6.0 Hz, 6H, Me<sup>ipr</sup>(*p*-cym)), 2.27 (s, 3H, Me<sup>Tol</sup>(*p*-cym)), 2.56 (s + m, 7H, Me<sup>dmbpy</sup>, CH<sub>ipr</sub>(*p*-cym)), 5.89 (d, *J* = 6.2 Hz, 2H, H<sup>3</sup>(*p*-cym)), 6.13 (d, *J* = 6.2 Hz, 2H, H<sup>2</sup>(*p*-cym)), 7.65 (d, *J* = 5.4 Hz, 2H, H<sup>5'</sup>), 8.24 (s, 2H, H<sup>3'</sup>), 9.30 (d, *J* = 5.8 Hz, 2H, H<sup>6'</sup>) ppm.

$[(\eta^6\text{-}p\text{-cymene})\text{Ru}(\text{OD}_2)(\text{dmbpy})]^{2+}(\mathbf{1b})$ . <sup>1</sup>H NMR (300 MHz, D<sub>2</sub>O, 298K): δ 0.89 (d, *J* = 7.7 Hz, 6H, Me<sup>ipr</sup>(*p*-cym)), 2.27 (s, 3H, Me<sup>Tol</sup>(*p*-cym)), 2.63 (s + m, 7H, Me<sup>dmbpy</sup>, CH<sub>ipr</sub>(*p*-cym)), 5.96 (d, *J* = 6.5 Hz, 2H, H<sup>3</sup>(*p*-cym)), 6.20 (d, *J* = 6.5 Hz, 2H, H<sup>2</sup>(*p*-cym)), 7.61 (d, *J* = 5.8 Hz, 2H, H<sup>5'</sup>), 8.19 (s, 2H, H<sup>3'</sup>), 9.36 (d, *J* = 5.8 Hz, 2H, H<sup>6'</sup>) ppm.

**Reaction of **1b** (18 mM) with HCOONa (180 mM).** An excess of HCOONa (6 mg, 9 × 10<sup>-2</sup> mmol) was added to a solution of **1a** (5 mg, 9 × 10<sup>-3</sup> mmol) in D<sub>2</sub>O (0.5 mL). The subsequent reaction was monitored by <sup>1</sup>H NMR spectroscopy during 24 h. Attempts to isolate the putative  $[(\eta^6\text{-}p\text{-cym})\text{Ru}(\text{D})(\kappa^2\text{-}N,N\text{-dmbpy})](\text{BF}_4)$  derivative failed, probably due to the high reactivity of this complex outside of the water medium.

$[(\eta^6\text{-}p\text{-cymene})\text{Ru}(\text{OOCH})(\text{dmbpy})]^+(\mathbf{1c})$ . <sup>1</sup>H NMR (300 MHz, D<sub>2</sub>O, 298K): δ 0.93 (d, *J* = 7.1 Hz, 6H, Me<sup>ipr</sup>(*p*-cym)), 2.09 (s, 3H, Me<sup>Tol</sup>(*p*-cym)), 2.56 (s, 6H, Me<sup>dmbpy</sup>), 5.88 (d, *J* = 5.9 Hz, 2H, H<sup>3</sup>(*p*-cym)), 6.19 (d, *J* = 5.9 Hz, 2H, H<sup>2</sup>(*p*-cym)), 7.65 (d, *J* = 5.4 Hz, 2H, H<sup>5'</sup>), 7.78 (s, 1H, HCOO), 8.12 (s, 2H, H<sup>3'</sup>), 9.38 (d, *J* = 6.9 Hz, 2H, H<sup>6'</sup>) ppm.

$[\text{Ru}(\eta^6\text{-}p\text{-cymene})(\text{D})(\text{dmbpy})]^+(\mathbf{1d})$ . <sup>1</sup>H NMR (300 MHz, D<sub>2</sub>O, 298K): δ 1.05 (d, 6H, Me<sup>ipr</sup>(*p*-cym)), 2.19 (s, 3H, Me<sup>Tol</sup>(*p*-cym)), 2.43 (s, 6H, Me<sup>dmbpy</sup>), 5.40 (d, *J* = 5.3 Hz, 2H, H<sup>3</sup>(*p*-cym)), 5.60 (d, *J* = 5.3 Hz, 2H, H<sup>2</sup>(*p*-cym)), 7.22 (d, *J* = 5.7 Hz, 2H, H<sup>5'</sup>), 7.96 (s, 2H, H<sup>3'</sup>), 8.67 (d, *J* = 5.7 Hz, 2H, H<sup>6'</sup>) ppm.

## ■ ASSOCIATED CONTENT

### ● Supporting Information

Kinetic information of the TH reactions for different substrates. Ratio calculation of isotopologues and isotopomers in the reaction products by GC–EI mass and <sup>13</sup>C NMR resonance assignment. Crystal data and structure refinement for complex **1a**. Cartesian coordinates, optimized structures, absolute energies, and Gibbs energies in water (Hartrees) of all the calculated species. Details of the pK<sub>a</sub> calculations. This material is available free of charge via the Internet at <http://pubs.acs.org>.

## ■ AUTHOR INFORMATION

### Corresponding Author

\*E-mail: Felix.Jalon@uclm.es.

### Notes

The authors declare no competing financial interest.

## ■ ACKNOWLEDGMENTS

This work was supported by the MINECO of Spain (projects CTQ2011-24434 and CTQ2011-2336, FEDER Funds). We thank the INCRECYT program of Castilla–La Mancha (contract to M.C.C.).

## ■ REFERENCES

- (1) (a) Atzrodt, J.; Derdau, V.; Fey, V.; Zimmermann, J. *Angew. Chem., Int. Ed.* **2007**, *46*, 7744–7765. (b) 10th International Symposium on the

Synthesis and Applications of Isotopes and Isotopically Labelled Compounds—Professor John R. Jones Memorial Lectures, Monday, June 15, 2009. *Label Compd. Radiopharm.* **2010**, 53, 227–238.

(2) (a) Lowry, T. H.; Richardson, K. S. *Mechanism and Theory in Organic Chemistry*; Harper and Row: New York, 1987. (b) *Synthesis and Application of Isotopically Labeled Compounds*; Pleiss, U., Voges, R., Eds; Wiley: New York, 2001; Vol. 7.

(3) (a) Junk, T.; Catallo, W. J. *J. Chem. Soc. Rev.* **1997**, 26, 401–406. (b) Saljoughian, M.; Williams, P. G. *Curr. Pharm. Des.* **2000**, 6, 1029–1056.

(4) Lieser, K. H. *Nuclear and Radiochemistry: Fundamentals and Applications*, 2nd ed.; Wiley-VCH: Weinheim, Germany, 2007.

(5) (a) Jensen, D. R.; Schultz, M. J.; Mueller, J. A.; Sigman, M. S. *Angew. Chem., Int. Ed.* **2003**, 42, 3810–3813. (b) Quinga, E. M. Y.; Mendenhall, G. D. *J. Am. Chem. Soc.* **1986**, 108, 474–478. (c) Erb, W. T.; Jones, J. R.; Lu, S. Y. *J. Chem. Res., Synop.* **1999**, 12, 728–729.

(6) (a) Liguori, A.; Mascaro, P.; Sindona, G.; Uccella, N. J. *Labelled Compd. Radiopharm.* **1990**, 28, 1277–1283. (b) Klomp, D.; Maschmeyer, T.; Hanefeld, U.; Peters, J. A. *Chem.—Eur. J.* **2004**, 10, 2088–2093. (c) Rasmussen, T.; Jensen, J. F.; Østergaard, N.; Tanner, D.; Ziegler, T.; Norrby, P. *Chem.—Eur. J.* **2002**, 8, 177–184. (d) Polavarapu, P. L.; Fontana, L. P.; Smith, H. E. *J. Am. Chem. Soc.* **1986**, 108, 94–99. (e) Andersson, P. G. *J. Org. Chem.* **1996**, 61, 4154–4156. (f) Xu, L.; Price, N. P. *J. Carbohydr. Res.* **2004**, 339, 1173–1178.

(7) (a) Fujita, M.; Hiayama, T. *Tetrahedron Lett.* **1987**, 28, 2263–2264. (b) Fujita, M.; Hiayama, T. *J. Org. Chem.* **1988**, 53, 5405–5415.

(8) Sreekumar, C.; Pillai, C. N. *Synthesis* **1974**, 7, 498–499.

(9) Young, C. M.; Skaddan, M. B.; Bergman, R. G. *J. Am. Chem. Soc.* **2004**, 126, 13033–13043.

(10) (a) Balzarek, C.; Tyler, D. R. *Angew. Chem., Int. Ed.* **1999**, 38, 2406–2408. (b) Balzarek, C.; Weakley, T. J. R.; Tyler, D. R. *J. Am. Chem. Soc.* **2000**, 122, 9427–9434. (c) Breno, K. L.; Tyler, D. R. *Organometallics* **2001**, 20, 3864–3868. (d) Klei, S. R.; Golden, J. T.; Tilley, T. D.; Bergman, R. G. *J. Am. Chem. Soc.* **2002**, 124, 2092–2093. (e) Sajiki, H.; Aoki, F.; Esaki, H.; Maegawa, T.; Hirota, K. *Org. Lett.* **2004**, 6, 1485–1487. (f) Takahashi, M.; Oshima, K.; Matsubara, S. *Chem. Lett.* **2005**, 34, 192–212. (g) Nishioka, T.; Shibata, T.; Kinoshita, I. *Organometallics* **2007**, 26, 1126–1128. (h) Esaki, H.; Aoki, F.; Umamura, M.; Kato, M.; Maegawa, T.; Monguchi, Y.; Sajiki, H. *Chem.—Eur. J.* **2007**, 13, 4052–4063. (i) Esaki, H.; Ohtaki, R.; Maegawa, T.; Monguchi, Y.; Sajiki, H. *J. Org. Chem.* **2007**, 72, 2143–2150. (j) Maegawa, T.; Fujiwara, Y.; Inagaki, Y.; Monguchi, Y.; Sajiki, H. *Adv. Synth. Catal.* **2008**, 350, 2215–2218. (k) Kurita, T.; Hattori, K.; Seki, S.; Mizumoto, T.; Aoki, F.; Yamada, Y.; Ikawa, K.; Maegawa, T.; Monguchi, Y.; Sajiki, H. *Chem.—Eur. J.* **2008**, 14, 664–673. (l) Tse, S. K. S.; Xue, P.; Lau, Ch. W. S.; Sung, H. H. Y.; Williams, I. D.; Jia, G. *Chem.—Eur. J.* **2011**, 17, 13918–13925. (m) Khaskin, E.; Milstein, D. *ACS Catal.* **2013**, 3, 448–452.

(11) Hou, G.; Gosselin, F.; Li, W.; McWilliams, J. Ch.; Sun, Y.; Weisel, M.; O'Shea, P. D.; Chen, Ch.-Yi; Davies, I. W.; Zhang, X. *J. Am. Chem. Soc.* **2009**, 131, 9882–9883.

(12) *Handbook of Homogeneous Hydrogenation* de Vries, J. G., Elsevier, C. J., Eds.; Wiley-VCH: Weinheim, Germany, 2007.

(13) (a) Cadierno, V.; Crochet, P.; Diez, J.; García-Garrido, S. E.; Gimeno, J. *Organometallics* **2004**, 23, 4836–4845. (b) Carrión, M. C.; Sepúlveda, F.; Jalón, F. A.; Manzano, B. R.; Rodríguez, A. M. *Organometallics* **2009**, 28, 3822–3833. (c) Ikariya, T.; Blacker, A. J. *Acc. Chem. Res.* **2007**, 40, 1300–1308. (d) Carrión, M. C.; Jalón, F. A.; Manzano, B. R.; Rodríguez, A. M.; Sepúlveda, F.; Maestro, M. *Eur. J. Inorg. Chem.* **2007**, 3961–3973. (e) Rautenstrauch, V.; Hoang-Cong, X.; Churlaud, R.; Abdur-Rashid, K.; Morris, R. H. *Chem.—Eur. J.* **2003**, 9, 4954–4967. (f) Noyori, R.; Ohkuma, T. *Angew. Chem., Int. Ed.* **2001**, 40, 40–73. (g) Wu, X. F.; Xiao, J. L. *Chem. Commun.* **2007**, 2449–2466. (h) Blaser, H. U.; Malan, C.; Pugin, B.; Spindler, F.; Steiner, H.; Studer, M. *Adv. Synth. Catal.* **2003**, 345, 103–151. (i) Chaloner, P. A.; Esteruelas, M. A.; Joo, F.; Oro, L. A. *Homogeneous Hydrogenation*; Kluwer Academic Publishers: Dordrecht, The Netherlands, 1994.

(14) (a) Wu, X.; Xiao, J. In *Metal-Catalyzed Reactions in Water*; Dixneuf, P. H., Cadierno, V., Eds.; Wiley-VCH: Weinheim, Germany,

2013; pp 173–242. (b) Wu, X.; Liu, J.; Di Tommaso, D.; Iggo, J. A.; Catlow, C. R. A.; Bacsá, J.; Xiao, J. *Chem.—Eur. J.* **2008**, 14, 7699–7715.

(15) (a) Coniglio, A.; Bassetti, M.; García-Garrido, S. E.; Gimeno, J. *Adv. Synth. Catal.* **2012**, 354, 148–158. (b) Cadierno, V.; Francos, J.; García-Garrido, S. E.; Gimeno, J. *Green Chem. Lett. Rev.* **2011**, 4, 55–61. (c) Dwars, T.; Oehme, G. *Adv. Synth. Catal.* **2002**, 344, 239–260.

(16) (a) Amrani, Y.; Lecomte, L.; Sinou, D. *Organometallics* **1989**, 8, 542–547. (b) Bakos, J.; Orosz, A.; Heil, B.; Laghmari, M.; Lhoste, P.; Sinou, D. *J. Chem. Soc., Chem. Commun.* **1991**, 1684–1685. (c) Lensink, C.; de Vries, J. G. *Tetrahedron: Asymmetry* **1992**, 3, 235–238. (d) Lensink, E.; Rijnberg, C.; de Vries, J. G. *J. Mol. Catal. A: Chem.* **1997**, 116, 199–207. (e) Wu, J.; Wang, F.; Ma, Y.; Cui, X.; Cun, L.; Zhu, J.; Deng, J.; Yua, B. *Chem. Commun.* **2006**, 1766–1768.

(17) Himeda, Y.; Miyazawa, S.; Onozawa-Komatsuzaki, N.; Hirose, T.; Kasuga, K. *Dalton. Trans.* **2009**, 32, 6286–6288.

(18) Wang, W.-H.; Hull, J. F.; Muckerman, J. T.; Fujita, E.; Hirose, T.; Himeda, Y. *Chem.—Eur. J.* **2012**, 18, 9397–9404.

(19) Türkmen, H.; Kani, I.; Çetinkaya, B. *Eur. J. Inorg. Chem.* **2012**, 4494–4499.

(20) (a) Rhyoo, H. Y.; Park, H. J.; Suh, W. H.; Chung, Y. K. *Tetrahedron Lett.* **2002**, 43, 269–272. (b) Bubert, C.; Blacker, J.; Brown, S. M.; Crosby, J.; Fitzjohn, S.; Muxworthy, J. P.; Thorpe, T.; Williams, J. M. J. *Tetrahedron Lett.* **2001**, 42, 4037–4039. (c) Rhyoo, H. Y.; Park, H. J.; Chung, Y. K. *Chem. Commun.* **2001**, 2064–2065. (d) Ma, Y. P.; Liu, H.; Chen, L.; Cui, X.; Zhu, J.; Deng, J. E. *Org. Lett.* **2003**, 5, 2103–2106.

(21) (a) Abura, T.; Ogo, S.; Watanabe, Y.; Fukuzumi, S. *J. Am. Chem. Soc.* **2003**, 125, 4149–4154. (b) Makihara, N.; Ogo, S.; Watanabe, Y. *Organometallics* **2001**, 20, 497–500. (c) Ogo, S.; Makihara, N.; Watanabe, Y. *Organometallics* **1999**, 18, 5470–5474.

(22) Aliende, C.; Pérez-Manrique, M.; Jalón, F. A.; Manzano, B. R.; Rodríguez, A. M.; Espino, G. *Organometallics* **2012**, 31, 6106–6123.

(23) (a) Nieto, I.; Livings, M. S.; Sacchi, J. B.; Reuther, L. E.; Zeller, M.; Papish, E. T. *Organometallics* **2011**, 30, 6339–6342. (b) Canivet, J.; Labat, G.; Stoeckli-Evans, H.; Süss-Fink, G. *Eur. J. Inorg. Chem.* **2005**, 4493–4500. (c) Romain, C.; Gaillard, S.; Elmkaddem, M. K.; Toupet, L. C.; Fischmeister, C. D.; Thomas, C. M.; Renaud, J.-L. *Organometallics* **2010**, 29, 1992–1995. (d) Canivet, J.; Karmazin-Brelot, L.; Süss-Fink, G. *J. Organomet. Chem.* **2005**, 690, 3202–3211. (e) Ogo, S.; Abura, T.; Watanabe, Y. *Organometallics* **2002**, 21, 2964–2969.

(24) (a) Seebach, D. *Angew. Chem., Int. Ed.* **1979**, 18, 239–258. (b) Gröbel, B. T.; Seebach, D. *Synthesis* **1977**, 6, 357–402.

(25) (a) Kuhn, F. E.; Santos, A. M.; Lopes, A. D.; Gonçalves, I. S.; Herdtweck, E.; Romao, C. C. *J. Mol. Catal. A: Chem.* **2000**, 164, 25–38. (b) Nunes, C. D.; Pillinger, M.; Hazell, A.; Jepsen, J.; Santos, T. M.; Madureira, J.; Lopes, A. D.; Gonçalves, I. S. *Polyhedron* **2003**, 22, 2799–280. (c) van Outersterp, J. W. M.; Stufkens, D. J.; Fraanje, J.; Goubitz, K.; Vlcek, A. *Inorg. Chem.* **1995**, 34, 4756–4766. (d) Gaballa, A.; Wagner, C.; Schmidt, H.; Steinborn, D. Z. *Anorg. Allg. Chem.* **2003**, 629, 703–710.

(26) Madern, N.; Talbi, B.; Salmain, M. *Appl. Organometal. Chem.* **2013**, 27, 6–12.

(27) Wang, L.; Pan, H.-R.; Yang, Q.; Fu, H.-Y.; Chen, H.; Li, R.-X. *Inorg. Chem. Commun.* **2011**, 14, 1422–1427.

(28) (a) Gladiali, S.; Alberico, E. *Chem. Soc. Rev.* **2006**, 35, 226–236. (b) Gladiali, S.; Mestroni, G. In *Transfer Hydrogenations in Transition Metals for Organic Synthesis: Building Blocks and Fine Chemicals*; Beller, M., Bolm, C., Eds.; Wiley-VCH: Weinheim, Germany, 1998; Vol. 2, pp 97–119.

(29) (a) Jiménez, M. V.; Fernández-Tornos, J.; Pérez-Torrente, J. J.; Modrego, F. J.; Winterle, S.; Cunchillos, C.; Lahoz, F. J.; Oro, L. A. *Organometallics* **2011**, 30, 5493–5508. (b) Chin, C. S.; Lee, B. J. *J. Am. Chem. Soc., Dalton Trans.* **1991**, 1323–1327. (c) Bellarosa, L.; Diez, J.; Gimeno, J.; Lledós, A.; Suárez, F. J.; Ujaque, G.; Vicent, C. *Chem.—Eur. J.* **2012**, 18, 7749–7765.

(30) (a) Liu, S.; Xiao, J. *J. Mol. Catal. A: Chem.* **2007**, 270, 1–43. (b) Barbaro, P.; Gonsalvi, L.; Guerriero, A.; Liguori, F. *Green Chem.* **2012**, 14, 3211–3219.

(31) Canivet, J.; Süss-Fink, G. *Green. Chem.* **2007**, 9, 391–397.

- (32) Creutz, C.; Chou, M. H.; Hou, H.; Muckerman, J. T. *Inorg. Chem.* **2010**, *49*, 9809–9822.
- (33) Busto, N.; Valladolid, J.; Aliende, C.; Jalón, F. A.; Manzano, B. R.; Rodríguez, A. M.; Gaspar, J. F.; Martins, C.; Biver, T.; Espino, G.; Leal, J. M.; García, B. *Chem. - Asian J.* **2012**, *7*, 788–801.
- (34) Hayashi, H.; Ogo, S.; Abura, T.; Fukuzumi, S. *J. Am. Chem. Soc.* **2003**, *125*, 14266–14267.
- (35)  $pD = pH$  meter reading + 0.4, Glasoe, P. K.; Long, F. A. *J. Phys. Chem.* **1960**, *64*, 188–190.
- (36) For cyclohexanone, see: Bordwell, F. G.; Fried, H. E. *J. Org. Chem.* **1991**, *56*, 4218–4223; For 3–pentanone: *J. Am. Chem. Soc.* **1975**, *97*, 7006–7014.
- (37) (a) Iron, M. A.; Ben-Ari, E.; Cohen, R.; Milstein, D. *Dalton Trans.* **2009**, 9433–9439. (b) Kovács, G.; Lledós, A.; Ujaque, G. *Organometallics* **2010**, *29*, 3252–3260. (c) Song, G.; Su, Y.; Periana, R. A.; Crabtree, R. H.; Hen, K.; Zhang, H.; Li, X. *Angew. Chem., Int. Ed.* **2010**, *49*, 912–917.
- (38) (a) Comas-Vives, A.; González-Arellano, C.; Corma, A.; Iglesias, M.; Sánchez, F.; Ujaque, G. *J. Am. Chem. Soc.* **2006**, *128*, 4756–4765. (b) Handgraaf, J.-W.; Meijer, E. J. *J. Am. Chem. Soc.* **2007**, *129*, 3099–3103. (c) Ariafard, A.; Asadollah, E.; Ostadebrahim, M.; Rajabi, N. A.; Yates, B. F. *J. Am. Chem. Soc.* **2012**, *134*, 16882–16890. (d) Jiménez-Tenorio, M.; Puerta, M. C.; Valerga, P.; Ortuño, M. A.; Ujaque, G.; Lledós, A. *Inorg. Chem.* **2013**, *52*, 8919–8932.
- (39) (a) Díez, J.; Gimeno, J.; Lledós, A.; Suárez, F. J.; Vicent, C. *ACS Catal.* **2012**, *2*, 2087–2099. (b) Pavlova, A.; Meier, E. J. *ChemPhysChem* **2012**, *13*, 3492–3496. (c) Dub, P. A.; Ikariya, T. *J. Am. Chem. Soc.* **2013**, *135*, 2604–2619.
- (40) Sunoj, R. B.; Anand, M. *Phys. Chem. Chem. Phys.* **2012**, *14*, 12715–12736.
- (41) (a) Rossin, A.; Kovács, G.; Ujaque, G.; Lledós, A.; Joó, F. *Organometallics* **2006**, *25*, 5010–5023. (b) Rossin, A.; Gonsalvi, L.; Phillips, A. D.; Maresca, O.; Lledós, A.; Peruzzini, M. *Organometallics* **2007**, *26*, 3289–3296. (c) Gancheff, J. S.; Kremer, C.; Denis, A.; Giorgi, C.; Bianchi, A. *Dalton Trans.* **2009**, 8257–8268. (d) Kovács, G.; Rossin, A.; Gonsalvi, L.; Lledós, A.; Peruzzini, M. *Organometallics* **2010**, *29*, 5121–5131.
- (42) Kelly, C. P.; Cramer, C. J.; Truhlar, D. G. *J. Phys. Chem. B* **2006**, *110*, 16066–16081.
- (43) (a) Soldevila-Barreda, J. J.; Bruijninx, P. C. A.; Habtemariam, A.; Clarkson, G. J.; Deeth, R. J.; Sadler, P. J. *Organometallics* **2012**, *31*, 5958–5967. (b) Kern, S.; van Eldik, R. *Inorg. Chem.* **2012**, *51*, 7340–7345.
- (44) (a) Comas-Vives, A.; Ujaque, G.; Lledós, A. *Adv. Inorg. Chem.* **2010**, *62*, 231–260. (b) Eisenstein, O.; Crabtree, R. H. *New J. Chem.* **2013**, *37*, 21–27.
- (45) (a) Martins, J. E. D.; Clarkson, G. J.; Wills, M. *Org. Lett.* **2009**, *11*, 847–850. (b) Soni, R.; Cheung, F. K.; Clarkson, G. C.; Martins, J. E. D.; Graham, M. A.; Wills, M. *Org. Biomol. Chem.* **2011**, *9*, 3290–3294.
- (46) The calculated  $pK_a$  of formic acid, using the theoretical approach described in the SI, is 3.1, which corresponds to a  $\Delta G_{\text{deprot}}$  of 4.2 kcal mol<sup>-1</sup>.
- (47) Cheung, F. K.; Lin, C.; Minissi, F.; Criville, A. L.; Graham, M. A.; Fox, D. J.; Wills, M. *Org. Lett.* **2007**, *9*, 4659–4662.
- (48) Ogo, S.; Kabe, R.; Hayashi, H.; Harada, R. *Dalton Trans.* **2006**, 4657–4663.
- (49) Åberg, J. B.; Samec, J. S. M.; Bäckwall, J.-E. *Chem. Commun.* **2006**, 2771–2773.
- (50) (a) Kovács, G.; Nádasdi, L.; Laurency, G.; Joó, F. *Green Chem.* **2003**, *5*, 213–217. (b) Kovács, G.; Schubert, G.; Joó, F.; Papai, I. *Organometallics* **2005**, *24*, 3059–3065.
- (51) Miyake, H.; Kano, N.; Kawashima, T. *J. Am. Chem. Soc.* **2009**, *131*, 16622–16623.
- (52) Ho, J. M.; Coote, M. L. *Theor. Chem. Acc.* **2010**, *125*, 3–21.
- (53) Bennett, M. A.; Huang, T.-N.; Matheson, T. W.; Smith, A. K.; Ittel, S.; Nickerson, W.; Fackler, J. F. *Inorg. Synth.* **1974**, *21*, 75.
- (54) Geary, W. J. *Coord. Chem. Rev.* **1971**, *7*, 81–122.
- (55) Zhao, Y.; Truhlar, D. *Theor. Chem. Acc.* **2008**, *120*, 215–241.
- (56) Frisch, M. J.; Trucks, G. W.; Schlegel, H. B.; Scuseria, G. E.; Robb, M. A.; Cheeseman, J. R.; Scalmani, G.; Barone, V.; Mennucci, B.; Petersson, G. A.; Nakatsuji, H.; Caricato, M.; Li, X.; Hratchian, H. P.; Izmaylov, A. F.; Bloino, J.; Zheng, G.; Sonnenberg, J. L.; Hada, M.; Ehara, M.; Toyota, K.; Fukuda, R.; Hasegawa, J.; Ishida, M.; Nakajima, T.; Honda, Y.; Kitao, O.; Nakai, H.; Vreven, T.; Montgomery, J. A., Jr.; Peralta, J. E.; Ogliaro, F.; Bearpark, M.; Heyd, J. J.; Brothers, E.; Kudin, K. N.; Staroverov, V. N.; Kobayashi, R.; Normand, J.; Raghavachari, K.; Rendell, A.; Burant, J. C.; Iyengar, S. S.; Tomasi, J.; Cossi, M.; Rega, N.; Millam, J. M.; Klene, M.; Knox, J. E.; Cross, J. B.; Bakken, V.; Adamo, C.; Jaramillo, J.; Gomperts, R.; Stratmann, R. E.; Yazyev, O.; Austin, A. J.; Cammi, R.; Pomelli, C.; Ochterski, J. W.; Martin, R. L.; Morokuma, K.; Zakrzewski, V. G.; Voth, G. A.; Salvador, P.; Dannenberg, J. J.; Dapprich, S.; Daniels, A. D.; Farkas, O.; Foresman, J. B.; Ortiz, J. V.; Cioslowski, J.; Fox, D. J. *Gaussian 09*, revision C.01; Gaussian, Inc.: Wallingford, CT, 2009.
- (57) Andrae, D.; Haeussermann, U.; Dolg, M.; Stoll, H.; Preuss, H. *Theor. Chim. Acta* **1990**, *77*, 123–141.
- (58) Ehlers, A. W.; Bohme, M.; Dapprich, M. S.; Gobbi, A.; Hollwarth, A.; Jonas, V.; Kohler, K. F.; Stegmann, R.; Veldkamp, A.; Frenking, G. *Chem. Phys. Lett.* **1993**, *208*, 111–114.
- (59) Hehre, W. J.; Ditchfield, R.; Pople, J. A. *J. Chem. Phys.* **1972**, *56*, 2257–2261.
- (60) Francl, M. M.; Pietro, W. J.; Hehre, W. J.; Binkley, J. S.; Gordon, M. S.; DeFrees, D. J.; Pople, J. A. *J. Chem. Phys.* **1982**, *77*, 3654–3665.
- (61) Marenich, A. V.; Cramer, C. J.; Truhlar, D. G. *J. Phys. Chem. B* **2009**, *113*, 6378–6396.
- (62) (a) Hratchian, H. P.; Schlegel, H. B. *J. Chem. Phys.* **2004**, *120*, 9918–9924. (b) Hratchian, H. P.; Schlegel, H. B. *J. Chem. Theor. Comput.* **2005**, *1*, 61–69.
- (63) SAINT+, version 7.12a. Area-Detector Integration Program. Bruker-Nonius AXS: Madison, Wisconsin, 2004.
- (64) Sheldrick, G. M. SADABS, version 2004/1. A Program for Empirical Absorption Correction. University of Göttingen: Göttingen, Germany, 2004.
- (65) SHELXTL-NT, version 6.12. Structure Determination Package. Bruker-Nonius AXS: Madison, Wisconsin, 2001.